

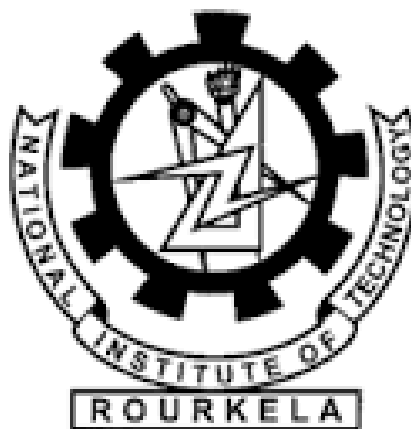
Reaction-sintered Alumina - Spinel Composites: Effect of Raw Material Sources

A thesis submitted in the partial fulfillment of the requirements for the
degree of Bachelor & Master of Technology in Ceramic Engineering

By

Shradha Suman Rickey

(710CR1130)



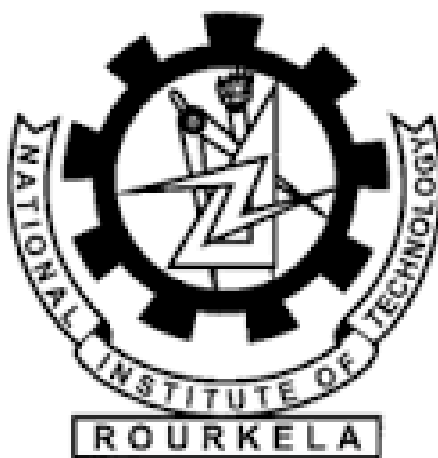
Reaction-sintered Alumina - Spinel Composites: Effect of Raw Material Sources

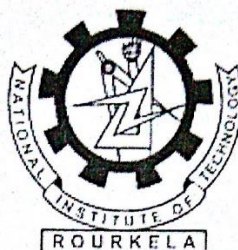
By

Shradha Suman Rickey

Under the supervision of

Prof. Ritwik Sarkar



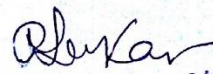


NATIONAL INSTITUTE OF TECHNOLOGY ROURKELA
CERTIFICATE

This is to certify that the thesis entitled, "Reaction-sintered Alumina - Spinel Composites: Effect of Raw Material Sources" submitted by *Ms. Shradha Suman Rickey (710CR1130)* in partial fulfilments for the requirements for the award of *Bachelor & Masters of Technology* degree in *Ceramic Engineering* at National Institute of Technology, Rourkela is an authentic work carried out by her under my supervision and guidance.

To the best of my knowledge, the matter embodied in this thesis has not been submitted to any other University/Institute for the award of any Degree or Diploma.

Date: 29/5/15


29/5/15

Dr. Ritwik Sarkar

Associate Professor

Department of Ceramic Engineering

National Institute of Technology

Rourkela – 769008

ACKNOWLEDGEMENT

With deep respect, I avail this opportunity to express my gratitude to Dr. Ritwik Sarkar, Associate Professor, National Institute of Technology, Rourkela for his inspiration and guidance and valuable suggestions throughout this research work. His vast knowledge in the field of Science and Technology has helped a lot to enlighten me. It would have been impossible on my part to come out with this project report without him.

I would like to express my gratitude to Dr. Swadesh Kumar Pratihara, HOD, Ceramic Engineering and all other faculties for constant support and valuable suggestions. I would also take this opportunity to express my gratitude to the non-teaching staff for their help and kind support. I am also thankful to the Research Scholars in the Department of Ceramic Engineering for helping out in labs and analysis.

Lastly I am thankful to my parents and friends who encouraged and constantly supported me during the total period of time and without whose support my project would not have been complete.

Date: 01/06/2015

Shradha Suman Rickey
710CR1130

ABSTRACT

The project involved the formation of alumina-spinel composites from combinations of different raw material sources, at two different compositions, varied over a range of temperatures succeeding a single stage firing route. The starting materials used were viz. A16SG, CL370, CT9FG for alumina sources and fused magnesia and sintered magnesia for magnesia sources. Alumina and magnesia sources were combined at compositions of 80:20 and 90:10 weight ratio, pressed and reaction sintered at temperatures 1200°C, 1300°C, 1400°C, 1500°C and 1600°C. Increase in the spinel content formed, was observed in samples fired at higher temperatures. Batches with finer raw material sources offered better densification an increasing trend with temperature was observed for the same. The XRD analysis plots of 80:20 batches showed trace amounts of corundum phase peaks at 1600°C while the 90:10 batches indicated small but clear peaks of the same at the highest temperature and that can be attributed to the higher residual alumina in the latter batches.

Contents

Chapter 1.....	8
Introduction	8
INTRODUCTION:.....	9
Ceramics in general:.....	9
Types:.....	10
Refractory industry & applications:	11
Spinel as a ceramic and refractory material:	13
Chapter 2.....	17
Literature Review	17
LITERATURE REVIEW:.....	18
Chapter 3.....	24
Objectives	24
OBJECTIVE:.....	25
Chapter 4.....	27
Experimental Procedure	27
EXPERIMENTAL PROCEDURE:	28
Raw materials used:.....	28
Instruments used:	29
Batch Preparation:	29
Preparation of samples by compaction:	30
Firing:	31
Characterizations:	32
Chapter 5.....	37
Results and Discussions	37
RESULTS & DISCUSSIONS:	38
Linear dimensional change after firing:	38

Bulk Density:	40
Apparent porosity:	42
Dilatometry:	43
XRD Analysis:	45
FESEM Analysis:	52
Chapter 6.....	56
Conclusion.....	56
CONCLUSION:	57
Chapter 7.....	58
References	58
REFERENCES:	59

Chapter 1

Introduction

INTRODUCTION:

Ceramics in general:

The word “ceramic” originated from the Greek word “Keramos” which means “Potters’ clay, tiles, pottery”. The most primitive ceramics, ever manufactured by the anthropoids, are pottery items, including 27,000 year old statuettes prepared from either pure clay or mixture of clay with silica, hardened, sintered, in fire. With time, the techniques matured, glazing and firing were performed over the body for a smoothened, designed and colored surface. Today the field of ceramics has widened to domestic, industrial and building products. It also has huge demand in the area of aesthetic applications.

Ceramic materials are usually hard, brittle, and chemically stable and non-conductors of heat and electricity but their properties may vary widely. For instance, while some of the ceramic compounds are extensively used to make electrical insulators, some are used as superconductors. So its properties expand the range of its application to a distant horizon.

The ceramic engineering deals with the techniques of their conversion from raw to the commercial scale. Thus it finds its use in almost all disciplines, mainly materials engineering, electrical engineering, chemical engineering and mechanical engineering. Other fields can be mining, aerospace, medicine, refinery, food and chemical industries, packaging science, electronics, industrial and transmission electricity, and guided lightwave transmission etc. There are many fields where the reach of ceramics covers a longer distance over metals and polymers for some of its special characteristics. Table. 1 follows in this regard.

Table 1 Comparison of some properties of ceramic, metal and polymer material

Property	Ceramic	Metal	Polymer
Hardness	Very High	Low	Very Low
Elastic modulus	Very High	High	Low
Thermal expansion	High	Low	Very Low
Ductility	Low	High	High
Corrosion resistance	High	Low	Low
Wear resistance	High	Low	Low
Electrical conductivity	Depends on material	High	Low
Density	Low	High	Very Low
Thermal conductivity	Depends on material	High	Low
Magnetic	Depends on material	High	Very Low

(N.B.: The table is for broad comparison purpose; specific properties depend on the material's specific composition and how it is made.)

Types:

Ceramics are broadly divided into two fields.

- a) Traditional ceramics
- b) Advanced ceramics

Traditional ceramics:

As per the name, traditional ceramics do not possess the rigid detailed and precise properties after their fabrication, so economical technologies are employed for most of the manufacturing processes. Ceramic materials like Ball clay, China clay, Feldspar, Silica, Dolomite, Talc, Calcite

and Nepheline form this group. In a traditional ceramic body, each of its components contributes a definite property to it. So choice of raw materials becomes crucial. Powder preparation is a crucial consideration in commercial ceramics. Surface area, particle size and distribution, particle shape, density, etc. each have their own contribution to production. Powder of required particle size, particle shape, and other requirements has to be prepared to meet the necessities for a particular industry. The powder need not be much pure as in case of advanced ceramics field. Pottery, tableware, sanitary ware, tiles, structural clay products, refractories, blocks, and electrical porcelain are some of the products of traditional ceramics.

Advanced ceramics:

Advanced ceramics are a distinct type of ceramics used mainly for electrical, electronic, optical, and magnetic applications. To guarantee that the manufactured ceramic powders own sufficient purity, advanced production techniques are implemented. Generally the production methods deals with chemical reactions to yield ceramic powder such as Sol-gel processing and liquid-gas reactions etc which makes most of them very expensive. Therefore, powder preparation has always stood as a cost factor in the advanced ceramics industry.

Refractory industry & applications:

According to ASTM C71 refractory materials are "non-metallic materials having those chemical and physical properties that make them applicable for structures, or as components of systems, that are exposed to environments above 1000 °F (811 K; 538 °C)." However as of today, this temperature has gone up dramatically. They are physically and chemically stable, and inert in the operating atmosphere. Thermal shock resistance is high enough to withstand the operating temperature. The main properties of refractories are:

- High temperature withstanding capacity
- High load bearing capacity
- Abrasion and wear resistance
- Erosion and corrosion resistance
- Higher thermal shock resistance

The main fields of applications are shown in Fig. 1 and its manufacturing method in Fig. 2.

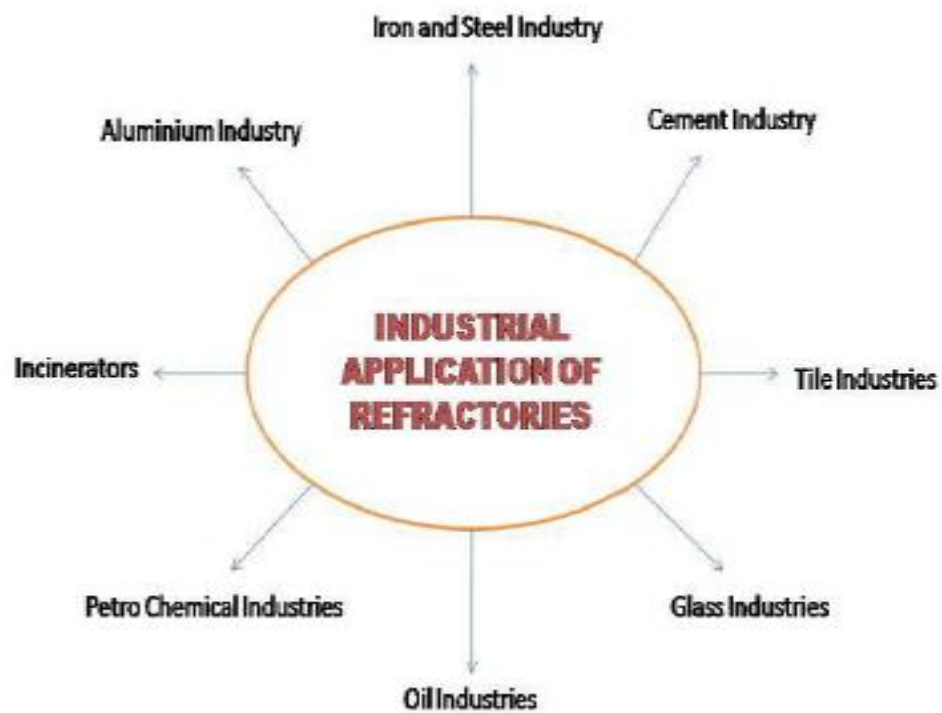


Figure 1 Applications of refractory

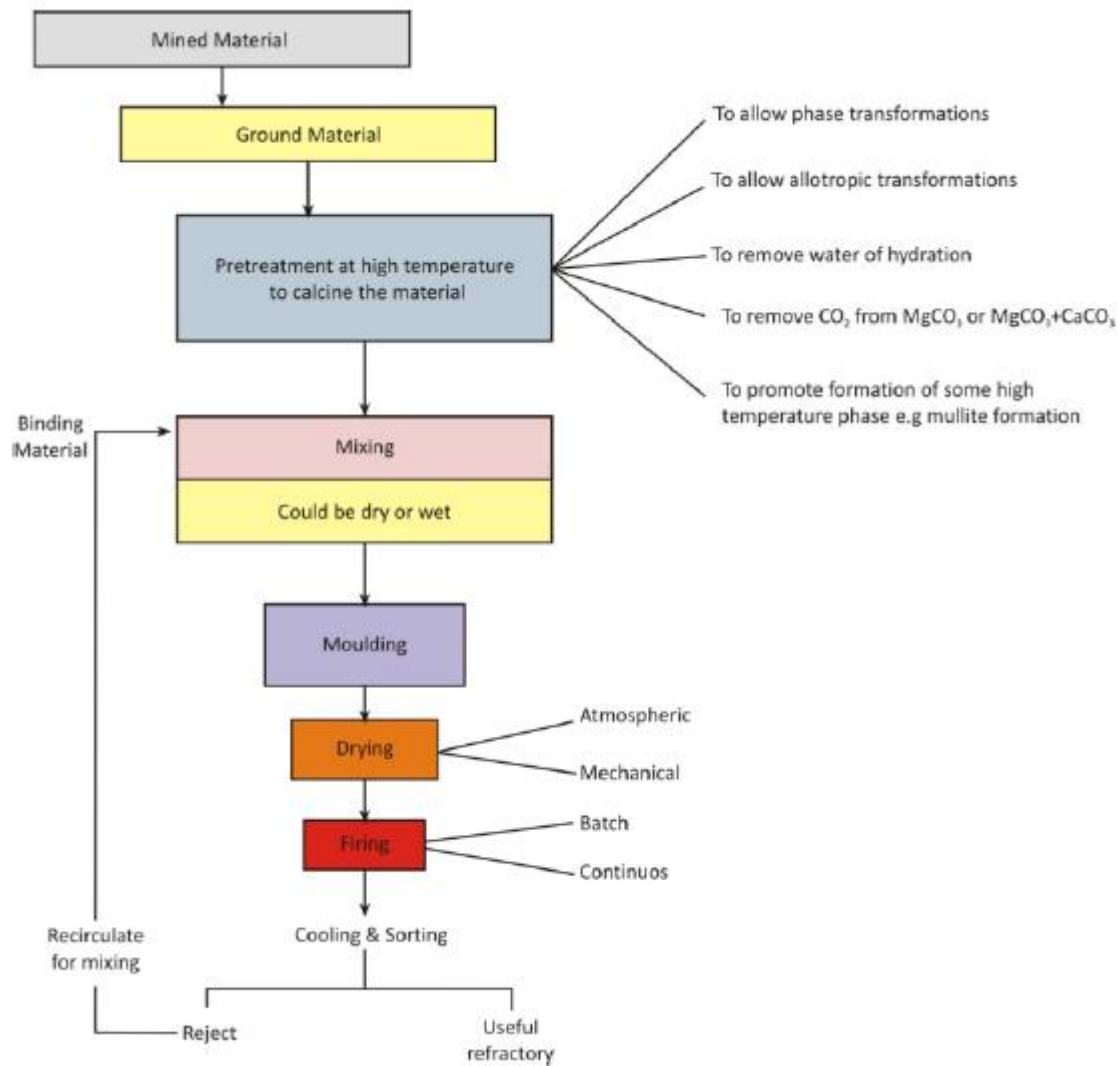


Figure 2 Manufacturing method of refractories

Some of the refractory varieties are fireclays, chromite, magnesite, high alumina, chromites, silicon carbide refractory etc.

Spinel as a ceramic and refractory material:

Introduction:

Magnesium aluminate spinel ($\text{MgO} \cdot \text{Al}_2\text{O}_3$) [Fig.3] is the parent member of chemical compound group with the common notation AB_2X_4 , where A and B represent bivalent and trivalent atoms

respectively, and X an anion such as O, S, Se or Te. On the basis the positioning of A and B atoms at the octahedral and tetrahedral sites, spinels are categorized in two parts.

(1) Normal; and (2) Inverse spinel.

Magnesium aluminate spinel can be categorized in three types on the basis of composition of magnesia (MgO) and alumina (Al₂O₃).

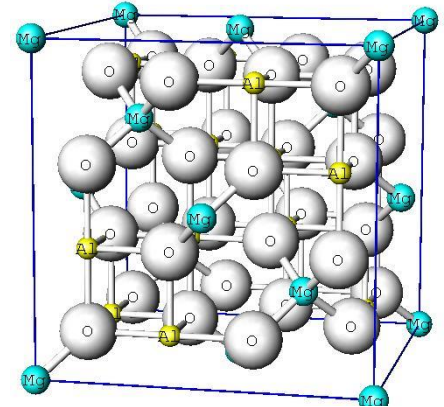


Figure 3 Structure of spinel

- (1) Stoichiometric: It contains 28% MgO and 72 % Al₂O₃.
- (2) Magnesia rich MgO.Al₂O₃ spinel: With excess MgO.
- (3) Alumina rich MgO.Al₂O₃ spinel: With excess Al₂O₃.

MA Spinel

Melting point (°C)	2135
Thermal expansion ($\times 10^{-6}/^{\circ}\text{C}$)	
100°C	5.6
500°C	7.6
1000°C	8.4
1500°C	10.2
Thermal conductivity (W/mK)	
25°C	15
100°C	13
500°C	8
1000°C	5
Density ($\text{g} \cdot \text{cm}^{-3}$)	3.58
Young's modulus (GPa)	240–284
Bending strength (MPa),	
RT	110–245
1400°C	8–10
Hardness (GPa)	15

Figure 4 Properties of Magnesium-aluminate spinel

Spinel with a higher melting temperature (2135°C) than Al₂O₃ (2054°C) and lower than MgO (2850°C) has its thermal expansion coefficient ($8.4 \times 10^{-6}/\text{K}$) very close to the value of alumina

($8.8 \times 10^{-6}/K$), but much lower than MgO ($13.5 \times 10^{-6}/K$). Due to its higher hydration resistance than periclase it can also be used in water-based castable systems.

The property of a refractory mostly relies upon nature, shape, size and conveyance of grains and pores, so pureness of raw material is fundamental to achieve helpful refractory properties.

Refractory property can likewise be enhanced by utilizing a substitute technique that comprises carefully designing and assemblage of phases or microstructure, distribution of lower melting phases, analysis of chemical and physical character of bond etc.

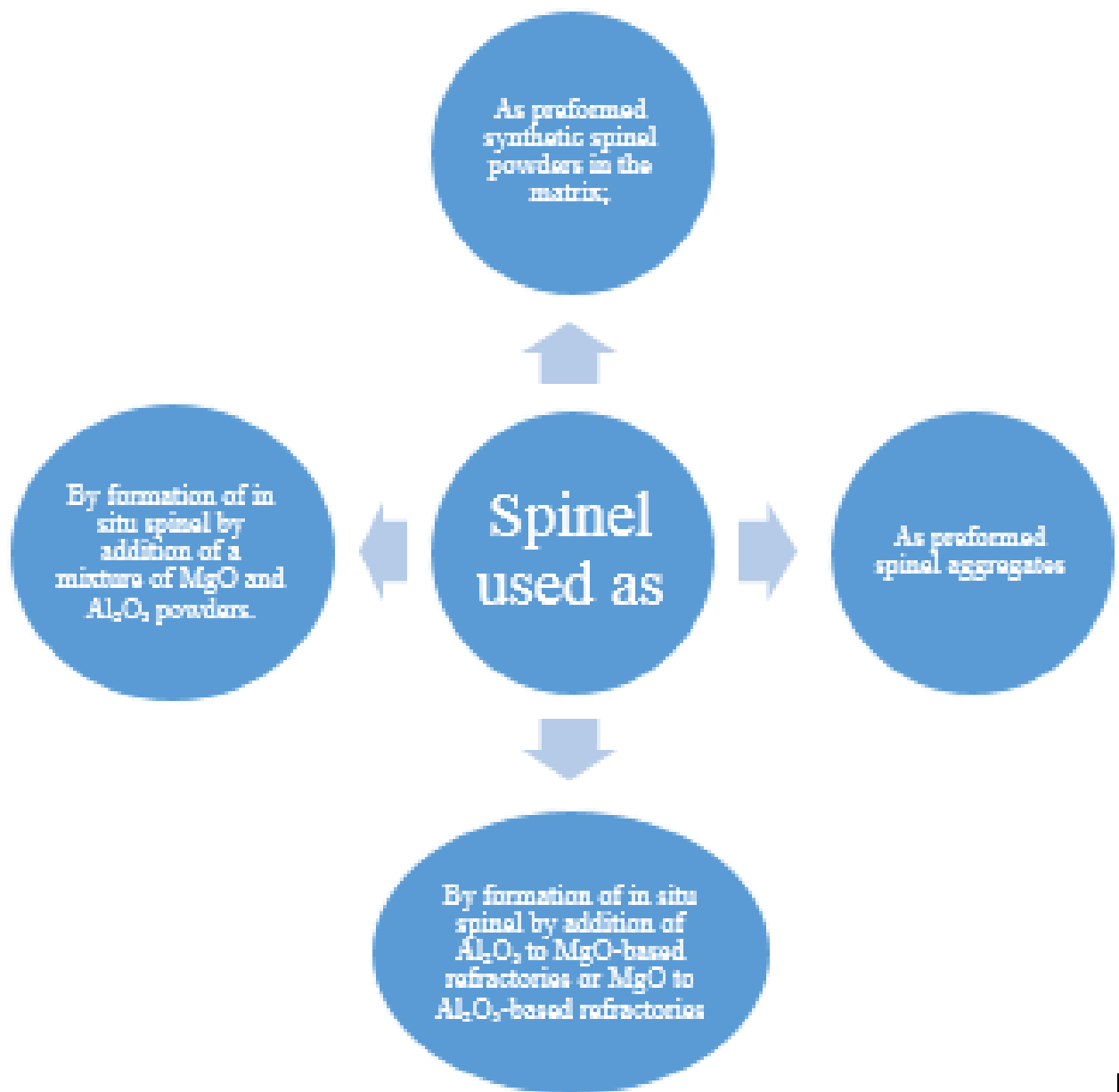
However, requirement of exceedingly pure raw materials as well as the processing costs makes it commercially expensive for industrial usage. A solid state reaction of the oxide reactants through counter diffusion process of Mg^{2+} and Al^{3+} ions in a rigid oxygen lattice is however a commercially acceptable production route (Fig. 5). However, as this method results in about 5% volume expansion which suppresses the sintering process [3], a two-stage firing method is adopted making the over-all process highly costly. Despite all this, the magnesium-spinel refractory has been able to attract much favor as the substitutes have failed at either efficiency or eco-friendly angle.

Application:

Magnesium aluminate spinel ($MgAl_2O_4$) has always stood as a remarkable refractory oxide of vast industrial significance in the field of structural ceramics. Its helpfulness is reflected in its valuable physical, chemical and thermal properties [Fig.4], both at standard and raised up temperatures. It has a congruent melting point of $2135^\circ C$, displays strong resistance to attack by most of the acids and alkalis & possesses small electrical losses. The range of applications of magnesium aluminate spinel refractory has thus widened in the areas of structural, chemical,

optical and electrical industry. This has its use in the refractory sidewalls and bottom of steel-ladle, transition and burning zones of cement rotary kilns, checker work of the glass furnace regenerators and many more.

Spinel is introduced into refractories in the following ways [10]:



Chapter 2

Literature Review

LITERATURE REVIEW:

Magnesium aluminate spinel does not occur naturally and so an efficient method needs to be used for its commercial scale production. The most ancient, easiest, but still extensively used method is the conventional oxide mixing (CMO), or solid – solid reaction, technique in which powder MgO- and Al₂O₃-bearing compounds (e.g., oxides, hydroxides, or carbonates) are mixed, shaped & sintered at high temperature for extended times. The resulting mass is pounded to powders of the preferred size distribution. Spinel formation via CMO has been explored comprehensively [9]. Initially, all the components needed to form the Magnesium aluminate product are spread homogeneously between particles of MgO and Al₂O₃. Hence small crystals with the spinel stoichiometry and structure are nucleated relatively simply on the exteriors of either MgO or Al₂O₃ grains. As soon as it's formed, as MgO and Al₂O₃ would no more be in interaction, rather separated by the impassable freshly formed spinel layer, further growth becomes tough. For the continuance of the reaction, a complex counter diffusion process ensues in which Mg²⁺ ions diffuse away from, and Al³⁺ ions diffuse toward, the MgO– MgAl₂O₄ interface and vice versa for the MgAl₂O₄–Al₂O₃ interface. Fig. can be referred to for a better understanding.

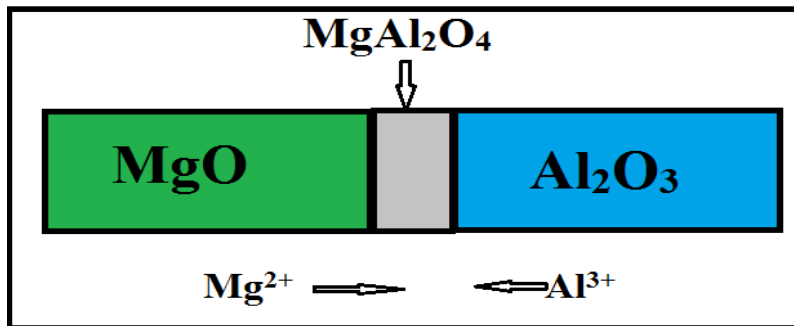


Figure 5 Counter diffusion process during MgAl₂O₄ formation

To placate local electro-neutrality throughout the product, every three Mg^{+2} ions that diffuse to the right-hand interface, two Al^{+3} ions must diffuse to the left-hand interface. The reactions that occur at the two interfaces may be written, ideally, as follows.

At the $\text{MgO}/\text{MgAl}_2\text{O}_4$ interface: $2\text{Al}^{+3} - 3\text{Mg}^{+2} + 4\text{MgO} = \text{MgAl}_2\text{O}_4$

At the $\text{MgAl}_2\text{O}_4 = \text{Al}_2\text{O}_3$ interface: $3\text{Mg}^{+2} - 2\text{Al}^{+3} + 4\text{Al}_2\text{O}_3 = 3\text{MgAl}_2\text{O}_4$

The overall reaction is: $4\text{MgO} + 4\text{Al}_2\text{O}_3 = 4\text{MgAl}_2\text{O}_4$

According to the equations, right-hand interface should move three times as quickly as the left-hand interface.

Spinel materialization becomes very slow by this process as ions like Mg^{+2} and Al^{+3} diffuse slowly. Defects are required, specially vacant sites into which adjacent ions can jump in.

Temperature should be high enough to impart sufficient thermal energy for occasional hop out of ions from one interstitial site or adjacent vacancy to another. Thus, it becomes problematic for solid-state spinel formation reactions to advance in the direction of a concluding point as the residual reactants become increasingly separated from each other. A general way of quickening the reactions is to recurrently regrind the incompletely reacted mixes, which acts to break up reactant– product interfaces and to fetch fresh reactant surfaces into contact so that the reactions can ensue yet again.

Alternatively, if gas- or liquid-phase aided passage of substance can take place, the reactants can be brought together without any necessity for long-range solid-state diffusion. A small quantity of gaseous or liquid transferring mediator, called mineralizer, may be effective in improving reaction rates. Effective mineralizers for spinel development reactions include fluorine- and boron-containing compounds viz. LiF , NaF , AlF_3 , Na_3AlF_6 and ZnF_2 , CaF_2 , BaF_2 , CaB_4O_7 ,

B₂O₃. These mineralizers can form liquid phases and/or help in creating cation vacancies, increasing spinel formation rate and decreasing its formation temperature.

The stoichiometric MgAl₂O₄ compound holds equimolar fractions of Al₂O₃ and MgO. However, spinel also exhibits a considerable amount of non-stoichiometry by deviating from its stoichiometric compositions. The incorporation of Al₂O₃ has been observed to be a lower energy process than that of MgO. The concentration of Aluminium and Magnesium cation vacancies is elevated in Al₂O₃ – rich spinel while excess magnesia is accommodated by a blend of oxygen vacancy and magnesium interstitial defects. [4] The magnesium aluminate spinel remains as a line compound in the Al₂O₃ – MgO phase diagram [Fig. 6] below 1300 K with exact equimolar proportions. At temperatures above this value, considerable amount of non-stoichiometry is observed [4]. Solubility extent varies for excess Al₂O₃ from excess MgO in spinel. Alumina, however, has higher solubility than magnesia.

The foremost application fields are transition and burning zones of cement rotary kilns, checker work of the glass furnace regenerators and side walls and bottom of the steel ladles [7].

Magnesia rich spinel with 66% alumina content has higher resistance to CO₂, SO₂, abrasion and corrosion and hence are used in cement rotary kiln.

Many works have been done [11-17] on the densifying behavior of stoichiometric and nonstoichiometric spinels. Bailey and Russel presented [11] a new 'partial reaction technique' for stoichiometric spinel where a combination of magnesia and alumina were calcined to finish 55 to 70% of spinellisation reaction, that permitted to overcome the limitation of 5% volume expansion while retaining adequate reactivity for a superior sintering on a second firing.

Teoreanu and Ciocea [12] attained better sintering in a single stage firing with calcined alumina and sintered magnesia, using MgCl₂ as a sintering aid. Comparatively pure kind of materials with

submicron particle sizes & sluggish rate of heating were found [13] to yield greatly densified magnesium aluminate spinel by using sea water magnesia and industry-grade alumina in a one-stage sintering procedure. For nonstoichiometric batch, Bailey and Russel [14] considered the system $\text{MgAl}_2\text{O}_4 \pm \text{Al}_2\text{O}_3$ using their own partial reaction technique [11]. They established a gradual fall in sintering with greater amount of alumina content up to 85 wt%. Alumina content above 85% was found to produce free corundum phase with increased density values. The same author [15] observed the excess magnesia (<10 wt%) in spinel composition was helpful for better densification, mechanical properties, controlled grain growth. Hing [16] reported density values of spinel close to theoretical density in both the non-stoichiometric magnesium aluminate spinel compositions by firing in a hydrogen atmosphere. He observed that the formation of vacancies in non-stoichiometric compositions enhanced the density values. Pal, Mukherjee and Samaddar found a confirmation from their study that the spinel can retain some quantity of alumina in its host structure even at room temperature, which may be exsolved as α -alumina during use, thus forming an interlocking structure between two types of (alumina and spinel) grains. Pressureless sintering study on excess alumina, stoichiometric, and excess magnesia spinel was done by Ching-Jui Ting and Hong-Yang Lu [18] in which he proposed oxygen lattice flow through vacancies to be the rate regulating mechanism for sintering of non-stoichiometric spinel compound. To find this they did a proportional study of the sintering rate derived from densification kinetics with the compositions examined when the concentration is converted to the activity of the two oxide constituents in MgAl_2O_4 which led them to the conclusion that the densification is occurring through a lattice diffusion mechanism in the solid state. Later they found the determined activation enthalpy to be close to the obtained value of oxygen self-diffusion derived in previous sintering studies.

A study of Ibram Ganesh and others [19] concluded that Stoichiometric and nonstoichiometric dense Magnesium Aluminate Spinel grains can be obtained by following a traditional double-stage process of firing from varied types of commercially obtainable alumina and magnesia as raw materials. Magnesia-rich (50 and 65 wt% Al_2O_3) and alumina-rich (90 wt% Al_2O_3) spinels might be sintered at 1650°C with soaking period of 1 h to attain equivalent properties as compared to those of materials existing in the market (for example ALCOA, USA). They also said that stoichiometric (72 by wt% Al_2O_3) dense Magnesium Aluminate Spinel grains with $\text{BD} > 43.30 \text{ g/cm}^3$, $\text{AP} < 2.0\%$, and $\text{WA} < 1.0\%$ could be produced from powders with $d_{50} < 5.0 \text{ mm}$ and a spinel phase containing $\sim 80\%$ by sintering at 1650°C for 1 h from compacts with a $\text{GD} \geq 1.96 \text{ g/cm}^3$. M.A.L. Braulio and others [21] reviewed the facts and information already existing for high-alumina spinel which contain castables (preformed and in situ) with the intention of providing a backing for innovative technological advances in the area. They considered the spinel content and grain size, the effect of calcium aluminate cement and hydratable alumina on the general castables possessions, the effect of different alumina and magnesia sources and the silica fume content as the prime variables. Mansour [22] has studied the effects of the characteristics of magnesia and alumina precursors on spinel formation. It is reported that the best condition for maximum spinel formation occurs when MgCO_3 is calcined at 900°C and $\text{Al}(\text{OH})_3$ is calcined at 1100°C for obtainment of the raw materials. Spinel formation also has been reported to be directly proportional with the crystal size of the reactants. Kostic et al. [23] have concluded that crushing energy increases the area of the surface and structural imperfections, and they have observed that continued grinding of starting materials resulted in spinel formation at lower temperatures.

According to Kong et al., [24] high-energy ball-milling of precursors decreases spinel formation at 900°C, and 98% densification is obtained by firing at 1550°C. Sarkar et al.[25] have described that alumina calcined at a temperature greater than 1600°C decreases the densification of magnesia-rich (66% alumina) spinel. Ikegami et al. [26] have reported that highly reactive low-temperature calcined powder, does not sinter well because of the existence of large amounts of rod like particles, which makes uniform compaction difficult. On the other hand, powder calcined at high temperature improves crystal growth and formation of hard agglomerates, which is accountable for poor sintered density.

Chapter 3

Objectives

OBJECTIVE:

The synthesis of spinel from its reactant oxide phases viz. MgO and Al_2O_3 , is accompanied with a volumetric expansion of 5%. Hence the popular manufacturing processes require a double-stage firing process for the complete spinelization reaction. This involves an initial calcination at around 1600°C and then crushing and milling, shaping and then a second firing to sinter the product and obtain a dense enough body. This process along with the maintenance of relevant parameters makes the method very costly [8]. This heavy expense for a refractory with highly alluring properties for industrial application demands for an extensive research in this field.

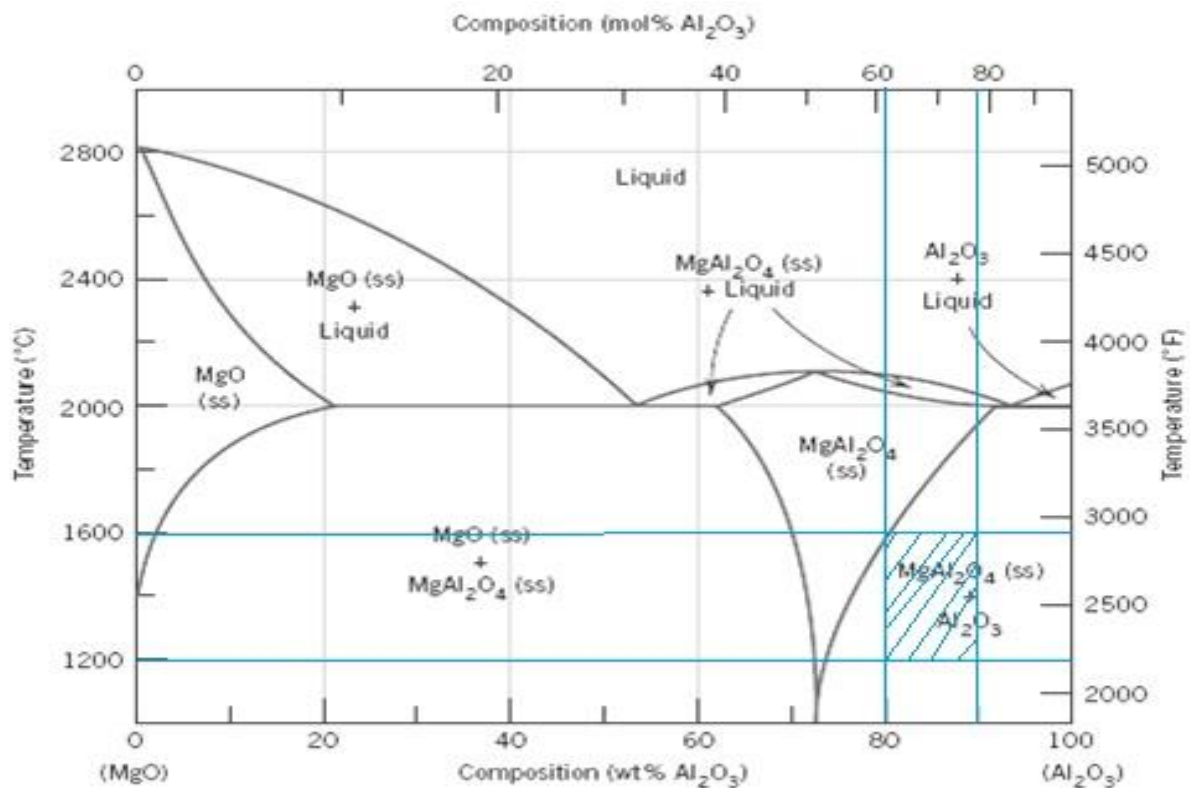


Figure 6 Phase diagram of MgO-Al₂O₃ demarcated with the working compositions

Here in this project, two alumina rich spinel systems, with $\text{Al}_2\text{O}_3:\text{MgO}$ wt % ratio at 80:20 and 90:10 were characterized. Sintering temperatures were chosen at values of 1200°C, 1300°C, 1400°C, 1500°C and 1600°C. From Fig. 6, we can see that the chosen parameters were supposed to form phases lying only in the demarcated region of the figure.

Chapter 4

Experimental

Procedure

EXPERIMENTAL PROCEDURE:

Raw materials used:

Alumina and magnesia of different commercial sources were used as the starting materials. The complete project dealt with combinations of three varieties of alumina and two of magnesia whose details have been listed in the table [Table. 2] below. All of the Alumina varieties were supplied by Almatris, India.

Table 2 Specifications of raw materials

Constituent	A16SG	CL370	CT9FG	Fused Magnesia	Sintered Magnesia
SiO ₂	0.05	0.06	0.03	0.47	0.12
Al ₂ O ₃	99.8	99.3		0.12	0.07
Fe ₂ O ₃	0.03	0.03	0.04	0.063	0.44
CaO	0.05	0.02	0.02	1.46	0.74
MgO	0.06	-	0.01	97.14	98.5
Na ₂ O+K ₂ O	0.14	0.14	0.15+	-	-
Sp. Surface Area (m ² /gm)	8.9	2.9	0.8	-	-
Average grain size (μm)	-	-		800	70
D ₅₀ (Cilas method) (μm)	0.51	2.5			
Grain Size Distribution	Mono-modal	Bi-modal	Mono-modal	-	-

Instruments used:

The project involved the use of a number of instruments for its successful completion. The details are mentioned below [Table. 3].

Table 3 Details of the Instruments used

Instrument Name	Used for	Company/Supplier name
Magnetic Stirrer	Mixing of batches	SPINOT Magnetic Stirrer
Drying oven	Drying	YORCO OVEN
Hydraulic Pressing Machine	Compaction	Carver Laboratory Press
High-temperature Furnace	Firing/Sintering	OKAY Electric Furnace
Weighing machine	Weighing	OHAUS Pioneer Balance
Dilatometer	Shrinkage analysis	NETZSCH TASC 414/4 Controller
X-Ray Diffractometer	Phase analysis	Philips PW 1730
FESE Microscope	Microstructure analysis	Nova NanoSEM
Muffle Furnace	Thermal etching	Testing Instruments,

Batch Preparation:

For the preparation of two non-stoichiometric batches, two compositions were chosen, one containing 80% Al_2O_3 and 20% MgO & another containing 90% Al_2O_3 and 10% MgO . The calculation for the batches were done using their corresponding percentage purity sheets and weighing was done with the help of OHAUS Pioneer Balance [Fig. 7]. The batches were prepared by mixing the raw materials in 100ml of iso-prpan-2-ol in the calculated proportions and then stirring the solution on a magnetic stirrer until the uniform mixing is achieved [Fig. 8].

The solutions were dried after mixing was complete for the removal of the liquid iso-propan-2-ol. The prepared batches were named as follows [Table. 4].

Table 4 Batch names

	80:20 Batch		90:10 Batch	
	Fused Magnesia	Sintered Magnesia	Fused Magnesia	Sintered Magnesia
A16SG	A1	A3	B1	B4
CL370	A2	A5	B2	B5
CT9FG	A3	A6	B3	B6



Figure 7 Weighing Balance



Figure 8 Batch making on magnetic stirrer

Preparation of samples by compaction:

The dried batch was mixed with 6% of 4% PVA (binder) and was compacted in a hydraulic-press machine [Fig. 9] under a load of 4 tonnes in a 15mm die-punch for obtaining the pellet

samples. The binder was intentionally organic in nature so that it goes off during drying. However the basic aim was to make the particles hold each other well after pressing and gain some green strength. The same process was followed for all the batches. The compacted green samples were kept in YARCO oven [Fig. 10] at 110°C for drying for 24 hours.



Figure 9 Hydraulic Press



Figure 10 Drying Oven

Firing:

Firing was performed at high temperatures with the purpose of achieving densification and spinalization. Temperature was varied over a range of 1200°C, 1300°C, 1400°C, 1500°C and 1600°C. This was done to study the effect of temperature on the same. 3 pellets from each of the 12 batches were kept on an unreactive alumina base plate, their positions were noted and put inside OKAY Electric Furnace [Fig. 11] programmed at the above said temperature values. The initial heating rate was kept low and later increased with the soaking period remaining constant at 2 hours for each of the firing temperature. The samples were allowed to cool for a daylong in the furnace itself after firing.



Figure 11 High temperature electric furnace

Characterizations:

Linear dimensional change after firing:

The original diameter of the samples before firing were measured to be 15mm. The diameters of the fired pellets were also measured. All the measurements were done using Vernier caliper. The measurements of the same batch samples were averaged for better precision.

The linear dimensional change after firing was found by using the following formula.

Linear dimensional change (in percentage) =

$$\frac{(\text{Diameter before sintering} - \text{Diameter after sintering}) * 100}{(\text{Diameter before sintering})}$$

A positive value indicated shrinkage whereas negative value was an indicative of expansion.

Apparent porosity & Bulk density calculation:

For the measurement of apparent porosity (AP) and bulk density (BD) of the sintered samples, Archimedes' principle was followed. Dry weight values of the samples were taken first. The samples were put in water and kept in a desiccator for 1-2 hours for vacuuming. The suspended weights were taken using a particular set-up apparatus and measurement of soaked weight followed. The suspended weight apparatus had a holder hanging into a beaker of water. The samples were placed on this holder and suspended weights were taken. For soaked weight measurement, the wet samples were put on a tissue paper so that the water only in the surface pores was removed. Finally the AP and BD values were obtained using the following formulae.

$$\text{Bulk density} = \frac{\text{Dry weight}}{\text{Soaked wt} - \text{Suspended wt}}$$

$$\text{Apparent porosity} = \frac{(\text{Soaked wt} - \text{Dry wt}) \times 100}{(\text{Soaked wt} - \text{Suspended wt})}$$

Dilatometry:

Sample making:

The batches were mixed with 4% PVA solution and bars of size 20*6 mm² were compacted using die-punch in the same hydraulic-press at a pressure of 2.5 tonnes. The green samples were polished on emery papers to obtain the optimum size required for the experiment to be done.

Dilatometry analysis:

Dilatometry was done using NETZSCH dilatometer [Fig. 12] up to a temperature of 1450°C. The graphs were plotted using Origin Pro 8.



Figure 12 Dilatometer set up

XRD Analysis:

X-Ray Diffraction was accomplished with Philips X-Ray diffractometer PW 1730 [Fig. 13] having nickel filtered Cu K α radiation ($\lambda=1.5406\text{\AA}$) by powder X-Ray diffraction technique. X-Ray powder diffraction method is a quick analytical technique used for identifications of phases of crystalline materials. The material to be analyzed has to be finely pounded and homogenized. The X-ray beam from the target material falls on the sample and diffraction occurs. The diffracted beams are collected, counted and processed by the detector. The sample is scanned through a range of 2θ angle so that all possible diffraction directions are covered due to the random orientation of sample particles [5]. Hence for the analysis, one from each of the sintered batch samples were crushed to powder using an agate mortar and submitted for XRD analysis. The rate was set to 20°C per min at a step size of 0.05 and scanned continuously in the range of 15° to 60° . The XRD results were analyzed using Xpert Highscore software.



Figure 13 X-Ray Diffractometer

FESEM:

Field emission scanning electron microscopy (FESEM) offers topographical and elemental facts at high amplifications of 10x to 300,000x, with nearly unlimited depth of field. Paralleled with Scanning Electron Microscopy (SEM), Field Emission SEM (FESEM) yields clearer, less electrostatically distorted images with spatial resolution down to 1-1/2 nanometers – three to six times better [6].

So one from each of the batch of the pellets sintered at 1600°C were polished and sent for FESEM (Field Effect Scanning Electron Microscope) [Fig. 14] analysis as polished surface would be able to expose grain boundaries of the body. The pellets were made to undergo rigorous polishing with first silicon sand papers of grading 1/0, 2/0, 3/0 and 4/0 and later with silicon carbide powder of grades of 400, 600 and 1000 on glass plates.

Diamond polishing had followed. It was done using diamond pastes holding diamond particles of the sizes of 10μ , 6μ and 1μ and a liquid spray. Thermal etching was performed to obtain more polish. The polished surfaced samples were submitted for FESEM experiment after gold coating.



Figure 14 FESEM Machine

Chapter 5

Results and

Discussions

RESULTS & DISCUSSIONS:

Linear dimensional change after firing:

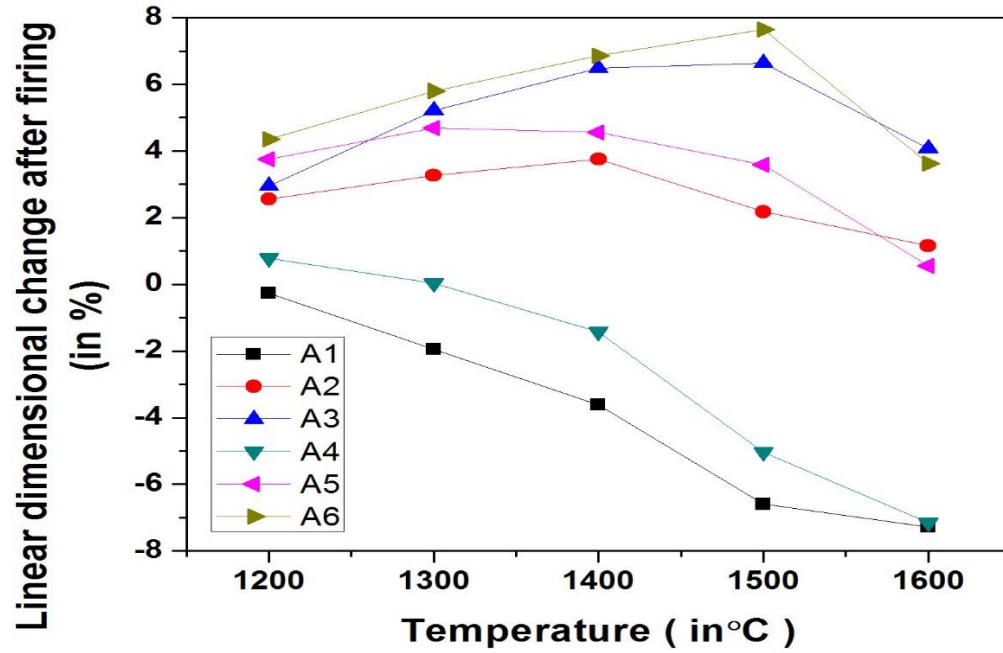


Figure 15 Linear dimensional change after firing of all 80:20 (A) composition batch

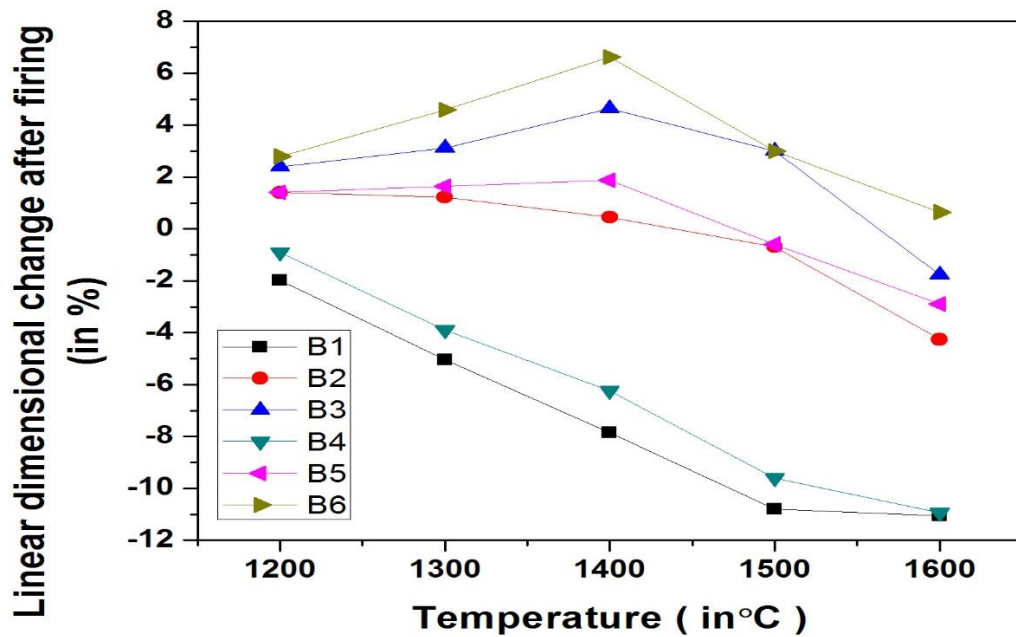


Figure 16 Linear dimensional change after firing of all 90:10 (B) composition batch

The dimensional changes observed after firing are shown in Fig. 15 and Fig. 16. Shrinkage has occurred for samples sintered at higher temperatures. A1 and A4, and B1 and B4 batches have shown only shrinkage and it has increased as the pellet is fired at higher temperature. The reason is the comparatively higher fineness of its component, A16SG alumina than the rest batches. This can be supported by the finding from the studies done by R. J. Brook and others, and J. P. Giry and others, separately, wherein the researchers found that densification depends on particles size of the starting material as L^{-3}/L^{-4} whereas the reaction depends as L^{-1}/L^{-2} where L symbolizes the particle size [2][20]. This relationship of densification and reaction with starting materials particle size in a reaction sintering system confirms that finer the size of the starting particles, densification will be pronounced compared to that of reaction between the reactants. However the absence of expansion doesn't render any information about the occurrence or extent of spinalization. Phase analysis may put some light on the fact in this regard. The higher expansions observed in cases of A2, A3, A5 and A6 indicates to a comparative inferior densification. Though the graphs tell about the starting of spinalization in their case, the extent can't be inferred from here. Same can be explained for the corresponding 90:10 (B) batches [Fig. 16]. The elevated values are evidencing the higher alumina content.

Bulk Density:

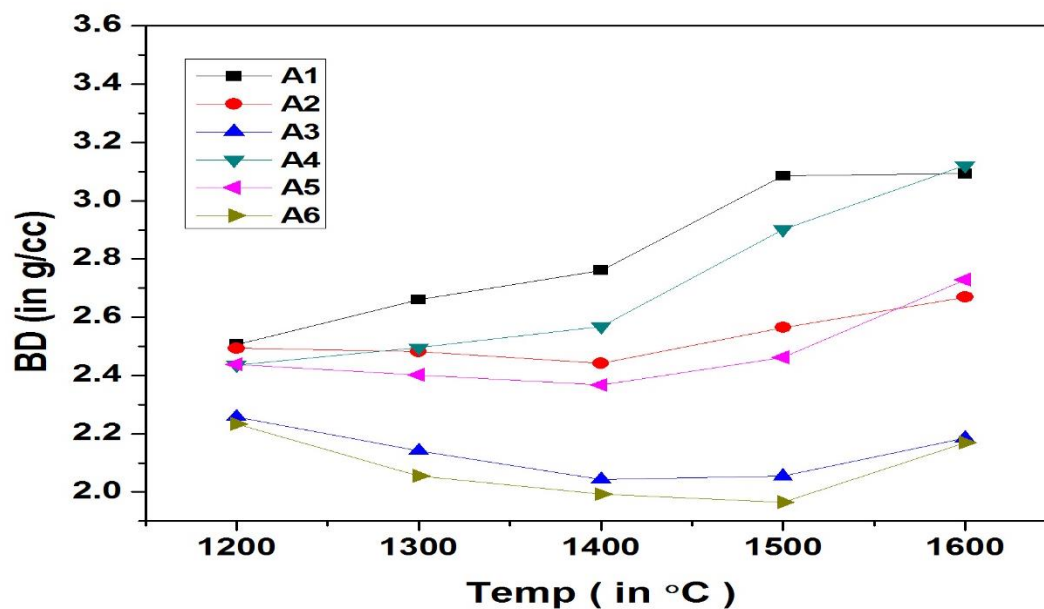


Figure 17 Bulk Density of the 80:20 (A) batches

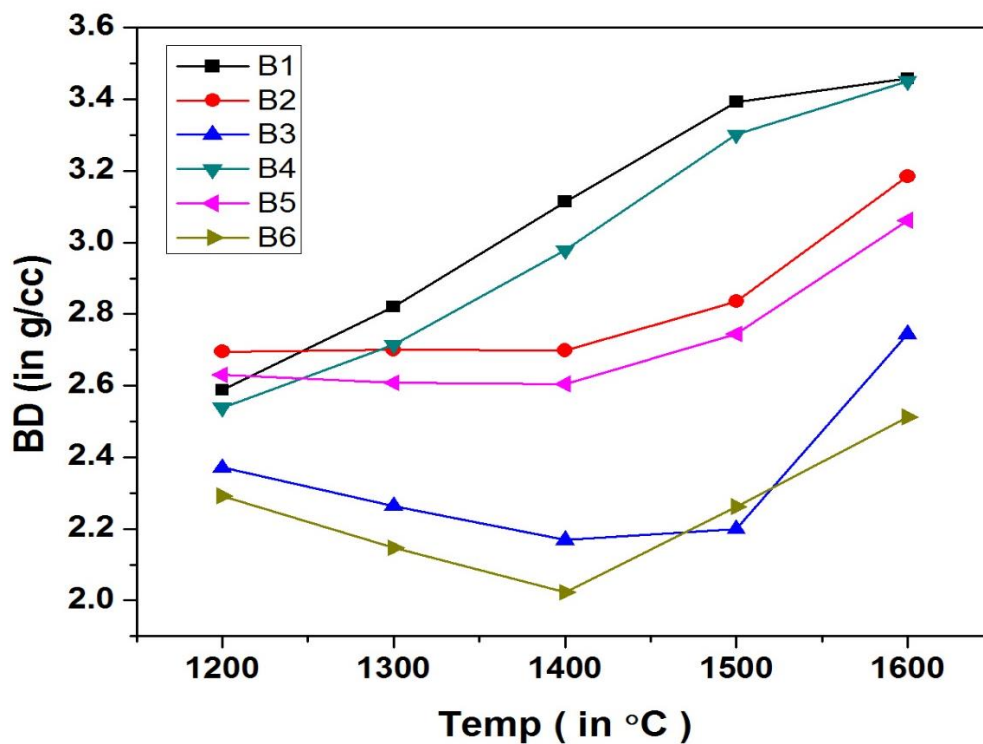


Figure 18 Bulk Density of the 90:10 (B) batches

The results of the BD experiment are plotted and shown in Fig. 17 and Fig. 18. The BDs for samples sintered at lower temperature are high and are becoming higher for the same sintered at higher temperatures in case of A1 and A4, and B1 and B4 batches. This can again be attributed to the higher sintering effect due to its higher fineness over the rest. For the rest of the batches, the BDs first decreased and then increased with the increase in the firing temperatures. The decrease in the BD values with increasing temperature is due to the increasing extent of spinel formation, associated with volume expansion(restricts any densification phenomenon). Once spinel formation is nearly completed at higher temperature, the densification starts and the BD values increase with increasing temperature. A distinct difference in the BD values were observed for samples containing different alumina sources. A16Sg containing samples were having higher density values, then the samples containing CL 370 and the least BD values were observed for the compositions with CT9FG samples. This trend of variatoin is associated with the fineness of the alumina source.

Also the absolute BD values of the B compositions were found to be higher than that of the A compositions due to higher amount of alumina and lesser extent of magnesia present in the compositions, resulting in lesser spinel formation and presence of free corundum phase has resulted in higher density values. But the trend in density values are exactly similar for both the A and B compositions.

Apparent porosity:

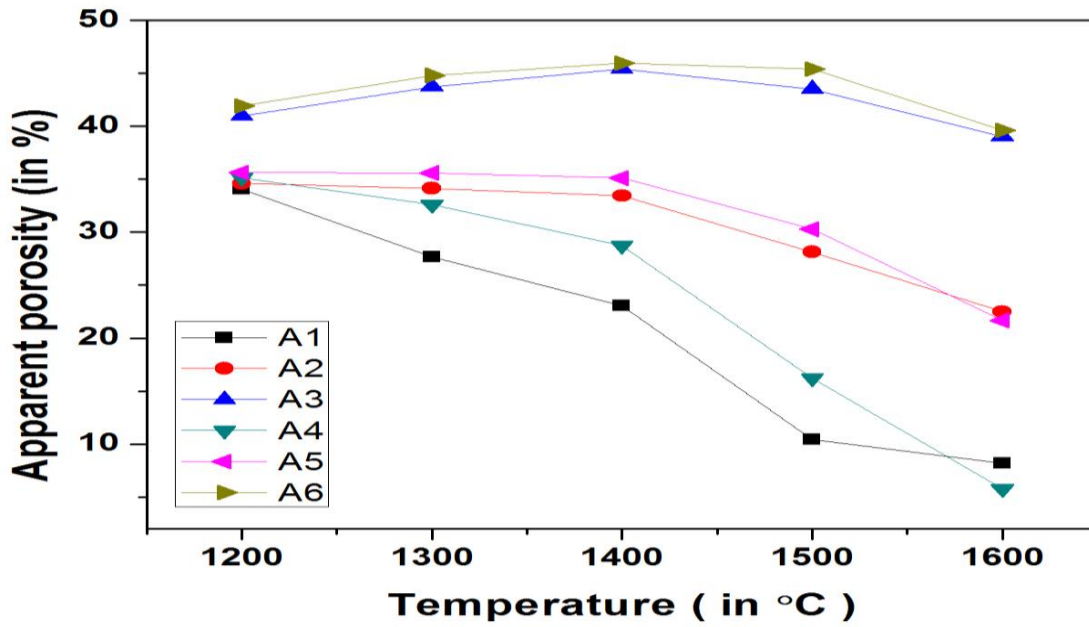


Figure 19 Apparent porosity of the 80:20 (A) batch

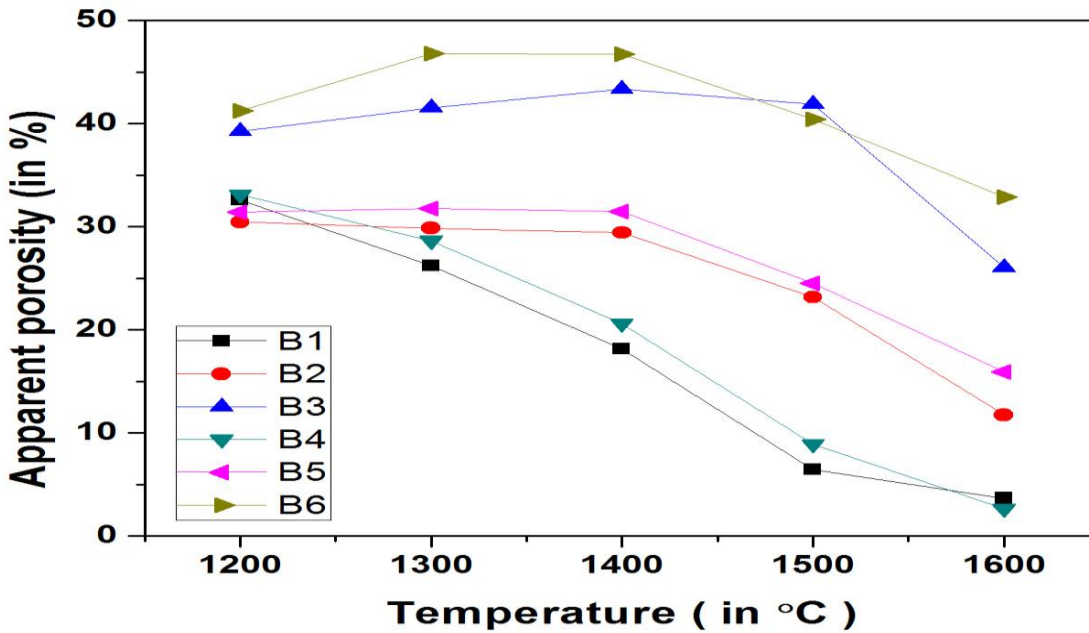


Figure 20 Apparent porosity of the 90:10 (B) batch

A1 and A4, and B1 and B4 are having quite low porosity in comparison with the rest of the batches as can be seen from the Fig. 19 and Fig. 20 for the better densification they have undergone. The other samples have shown higher porosity due to expansion and lesser sintering effect at lower temperatures. However the curves are showing a decreasing trend to the higher temperature side.

Dilatometry:

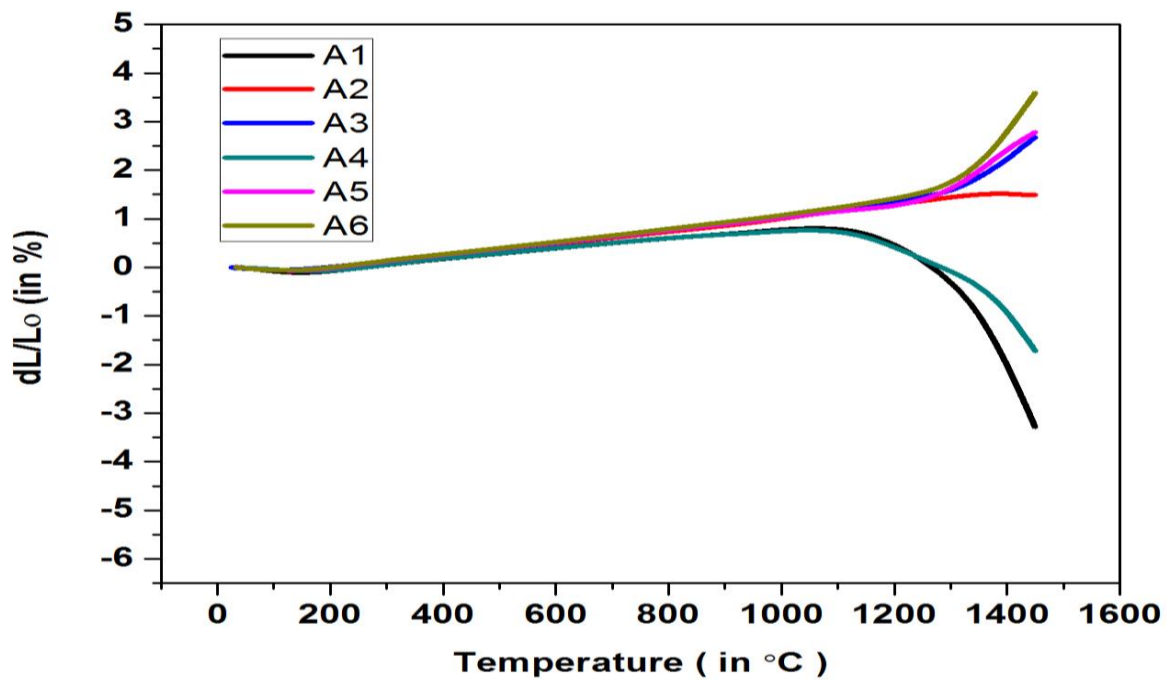


Figure 21 Dilatometric curves of 80:20 (A) batch

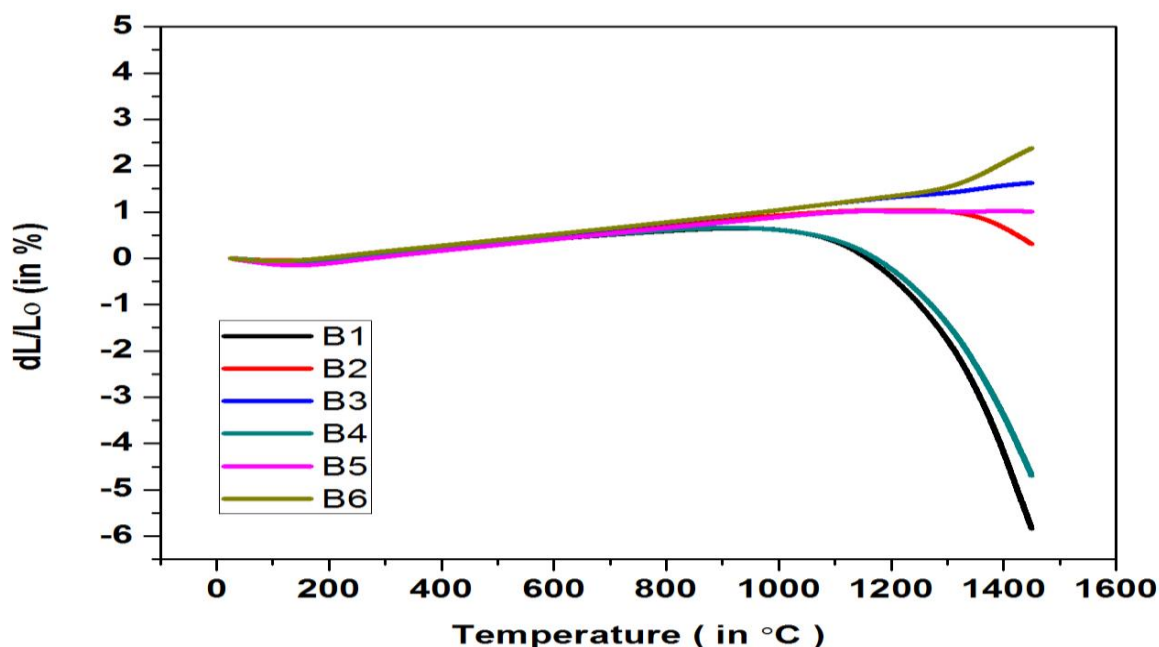


Figure 22 Dilatometric curve of 90:10 (B) batch

Dilatometric plots are given in containing the curves in Fig. 21 and Fig. 22 for A and B compositions respectively. In this study there are three different phenomena occurring, namely the reversal thermal expansion of the materials, the expansion due to spinel formation and the shrinkage due to densification and sintering of the compositions. Dilatometric study shows that there is a marginal increase in linear dimension of the samples with increasing temperature till about 1200°C, which is common for all the compositions. This may be associated with the reversal thermal expansion of the starting materials. After 1200°C the compositions having the higher surface area that is the composition with A16SG as source of alumina (A1, A4, B1 and B4) there is nearly no sudden increase in the thermal expansion values but a sharp and gradual decrease in linear dimension was observed with further increasing temperature. The decrease in dimension as observed for these compositions are because of the shrinkage in these compositions associated with the sintering that started at a lower temperature due to higher fineness of the compositions. Spinel formation is also obvious of these compositions but higher rate of

shrinkage due to densification from sintering was prominent and hence expansion behavior was not prominent for these compositions.

For other composition, there is a sharp increase in dimension above 1200°C which is associated with the spinel formation reaction. Higher the extent of spinel formation compared to the rate of shrinkage due to sintering will result a strong expansion peak and the highest expansion values were obtained for compositions A3, A6, B3 and B6 compositions. Nearly no shrinkage has occurred in these compositions which indicates poor sintering in these compositions. These compositions are also having the least densification values, as observed in the densification study, which supports the dilatometric behavior. Also the expansion values of the A compositions are higher than the B compositions due to higher extent of spinel formation in A compositions for higher extent of MgO present.

XRD Analysis:

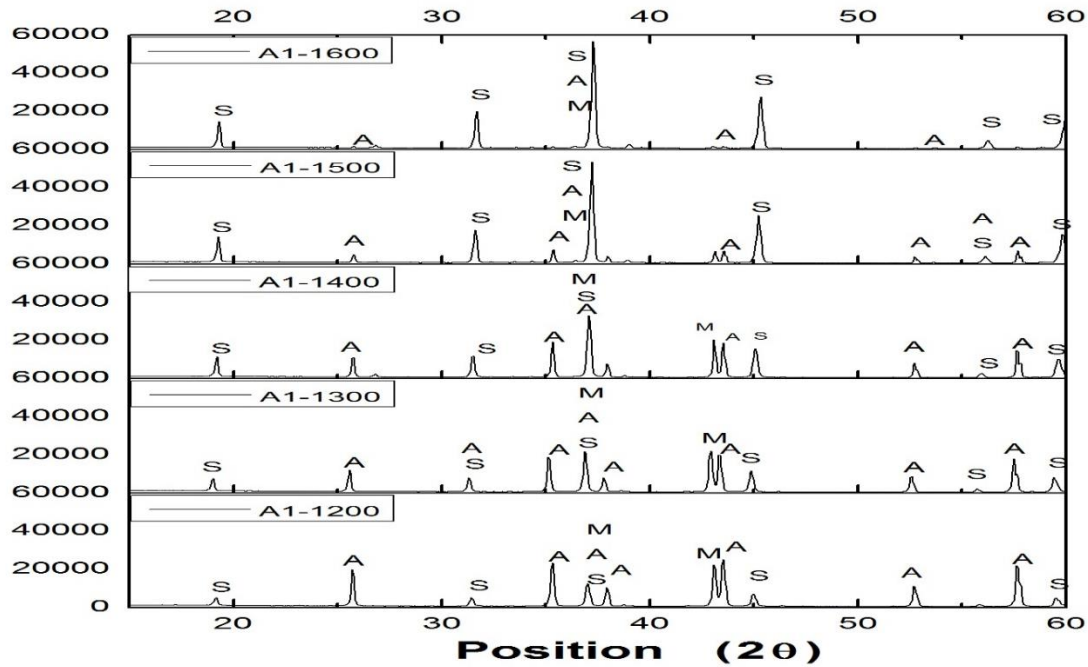


Figure 23 Comparison of XRD analysis plots of all A1 batches

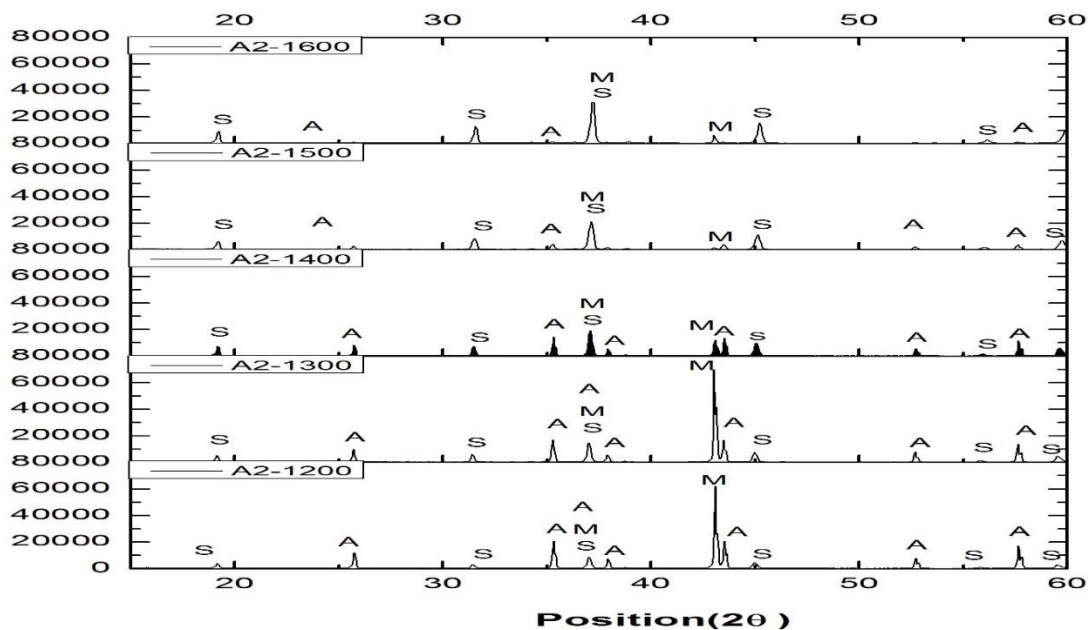


Figure 24 Comparison of XRD analysis plots of all A2 batches

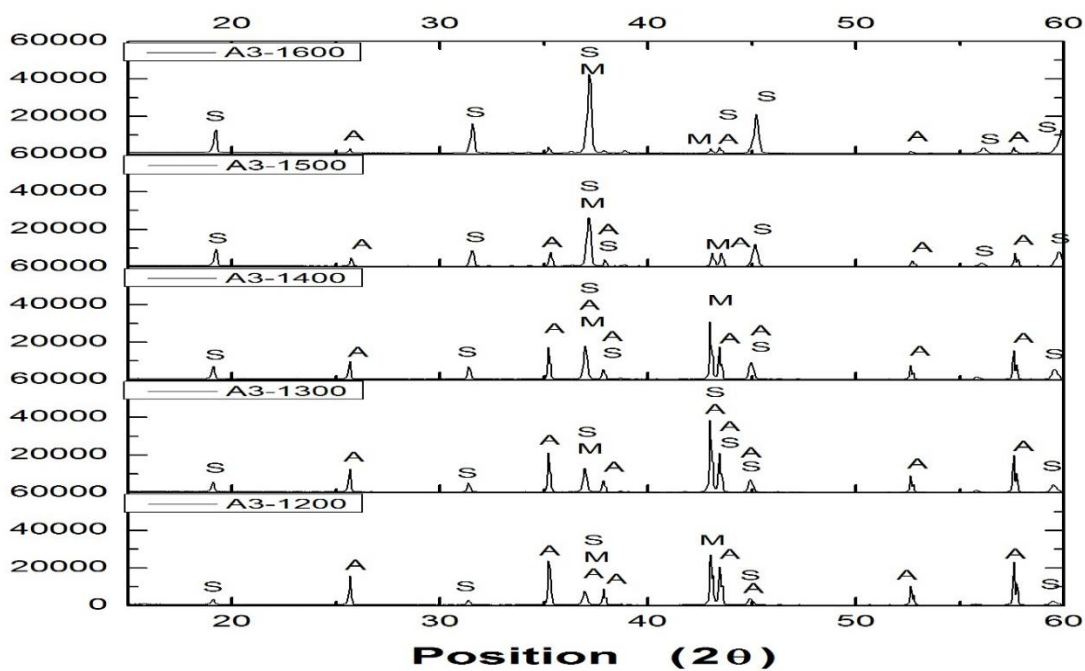


Figure 25 Comparison of XRD analysis plots of all A3 batches

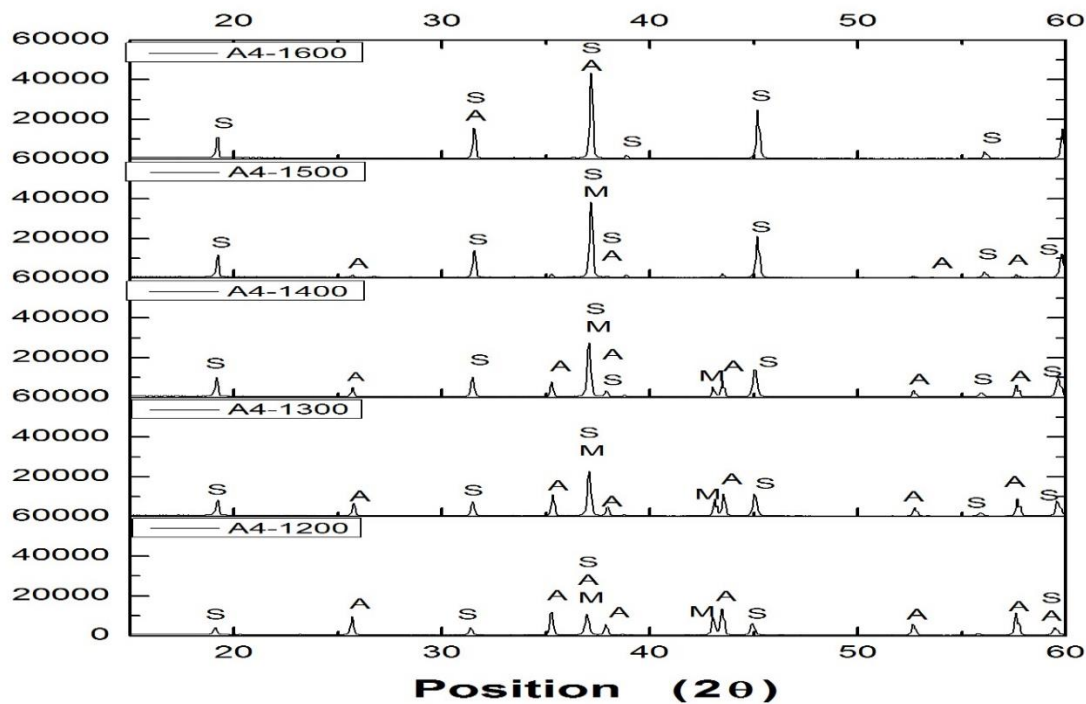


Figure 26 Comparison of XRD analysis plots of all A4 batches

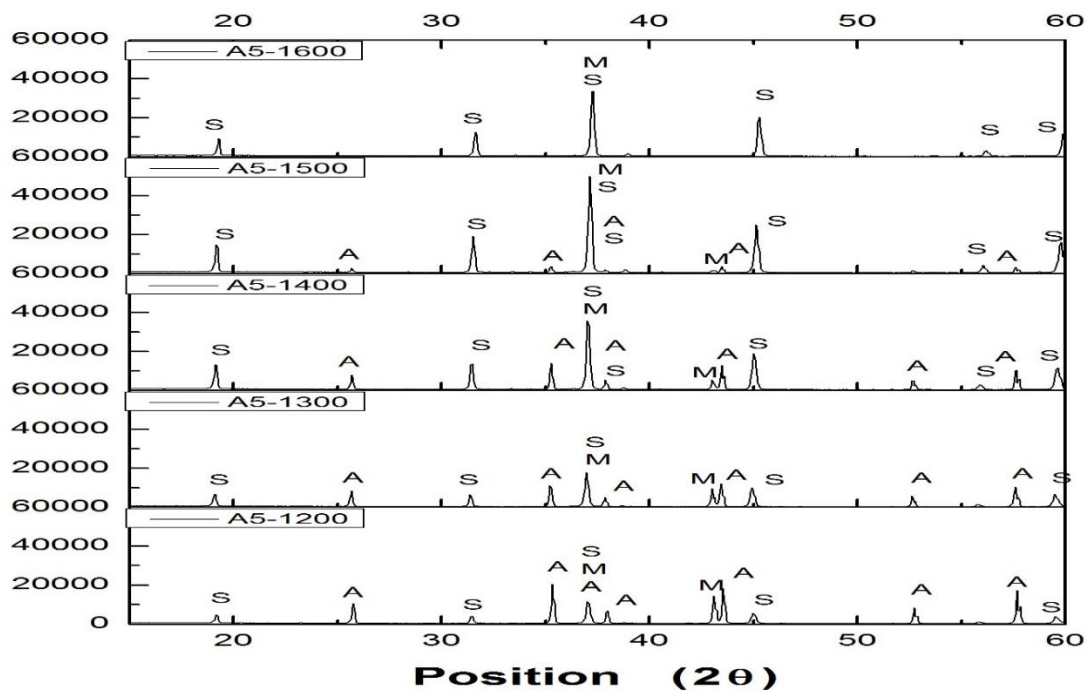


Figure 27 Comparison of XRD analysis plots of all A5 batches

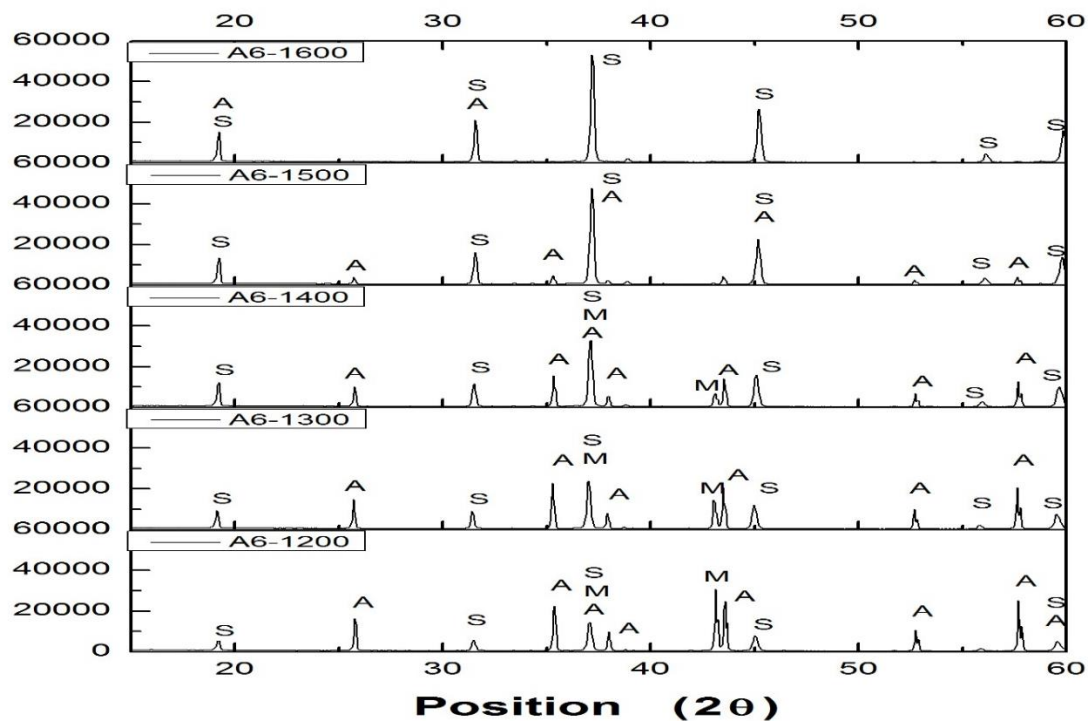


Figure 28 Comparison of XRD analysis plots of all A6 batches

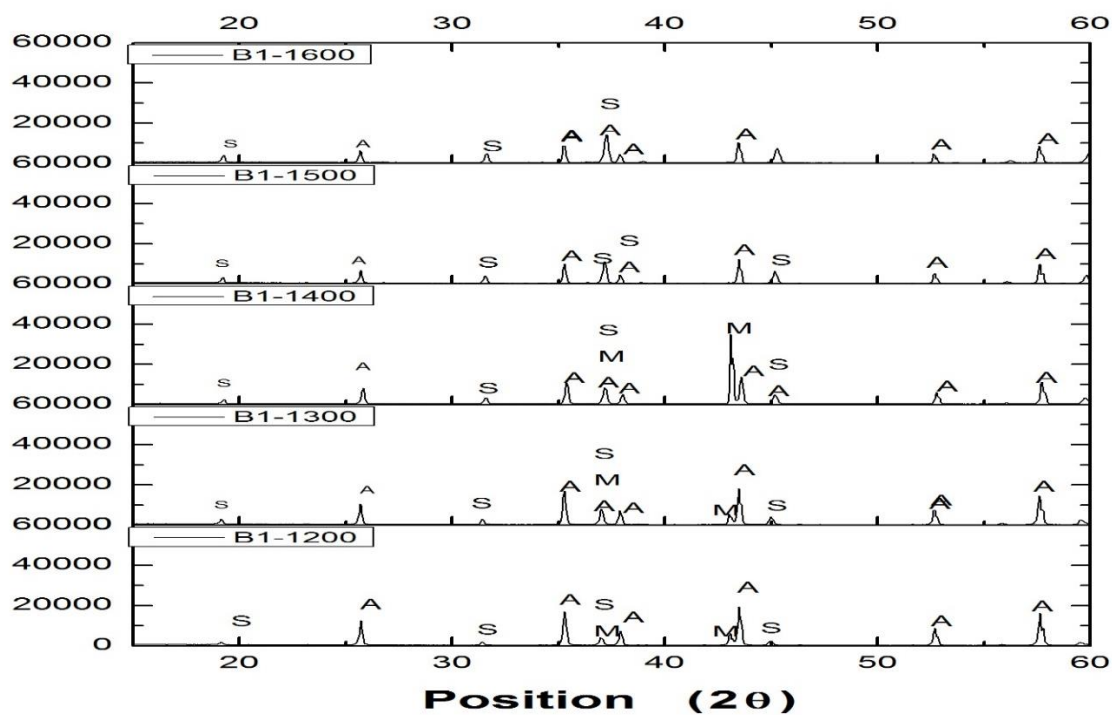


Figure 29 Comparison of XRD analysis plots of all B1 batches

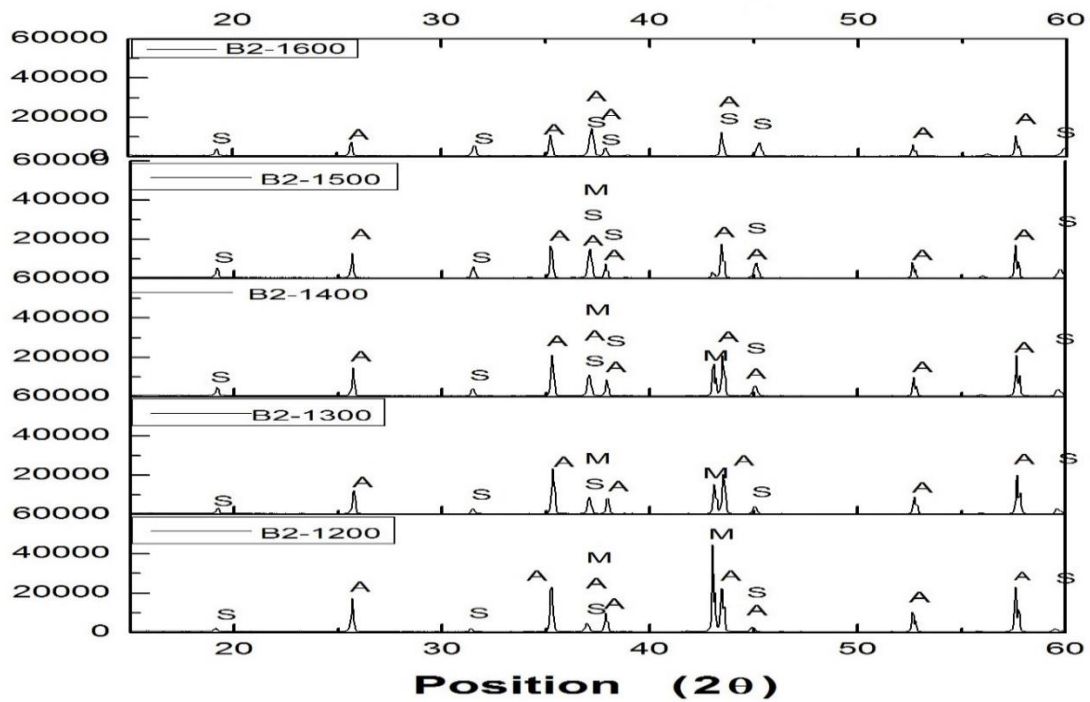


Figure 30 Comparison of XRD analysis plots of all B2 batches

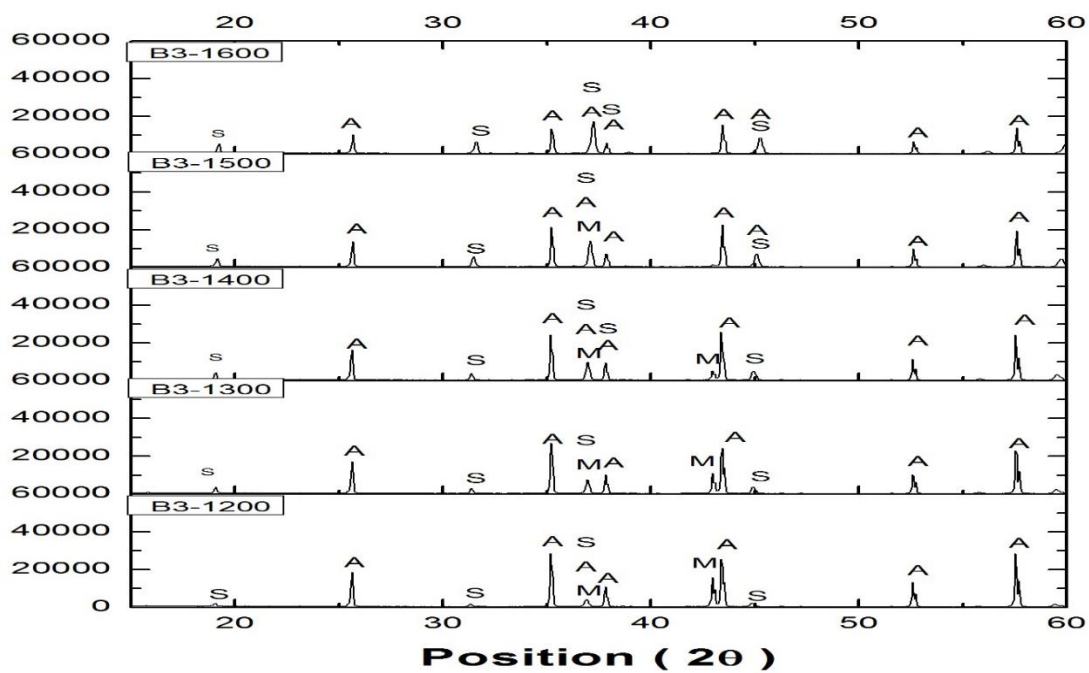


Figure 31 Comparison of XRD analysis plots of all B3 batches

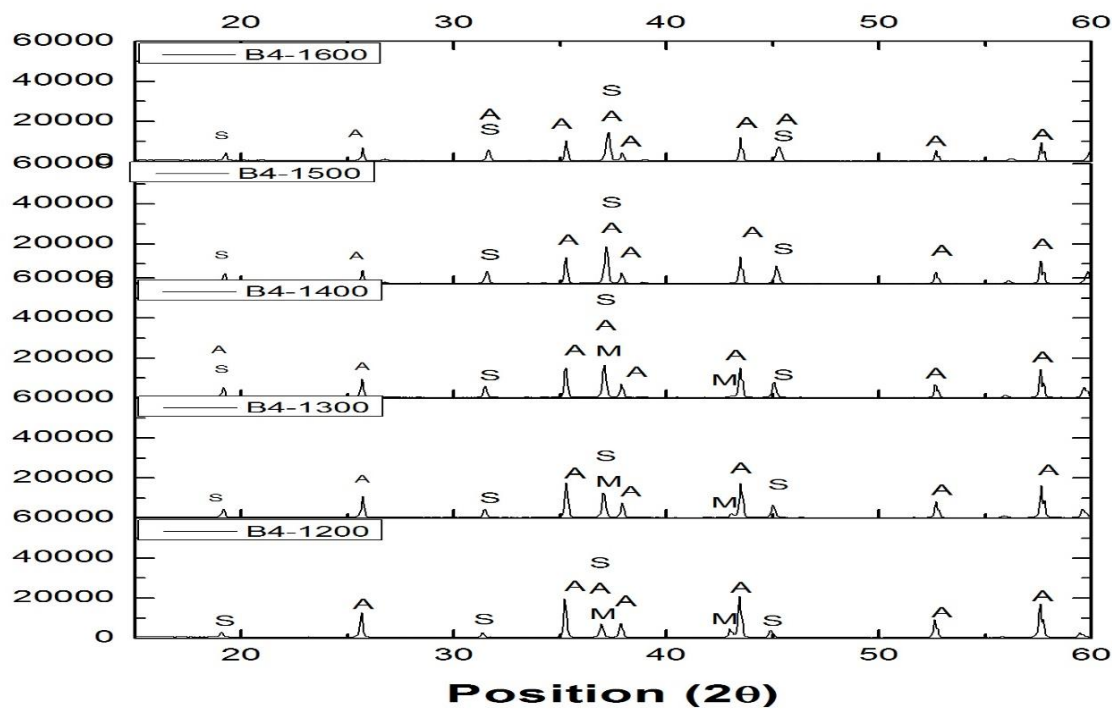


Figure 32 Comparison of XRD analysis plots of all B4 batches

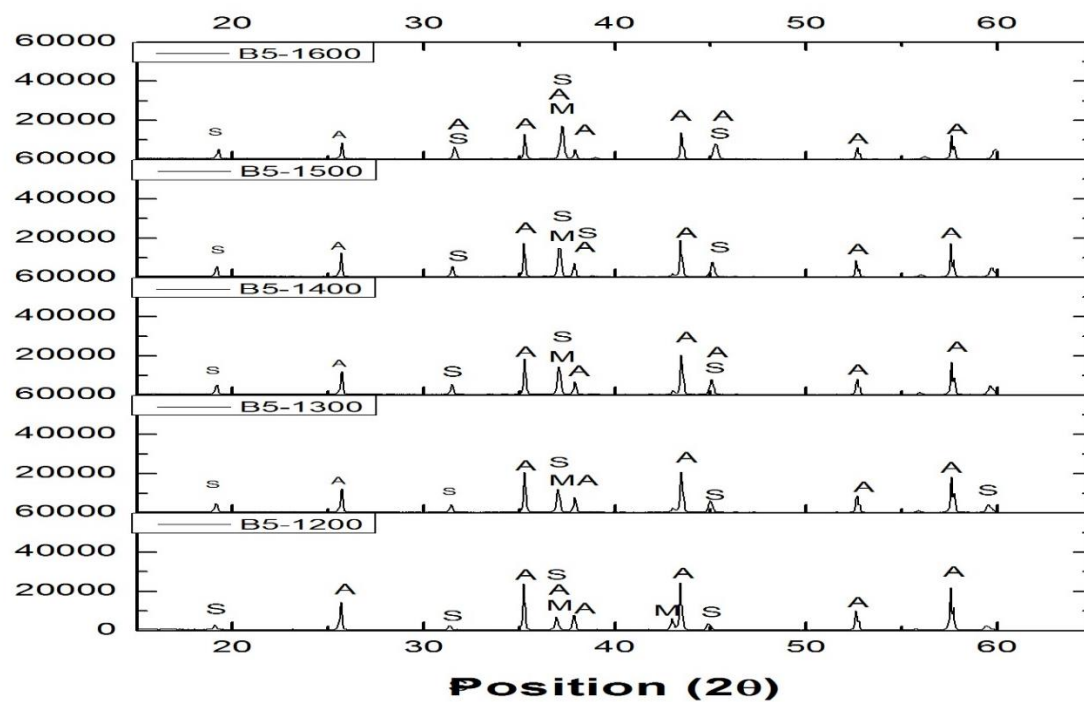


Figure 33 Comparison of XRD analysis plots of all B5 batches

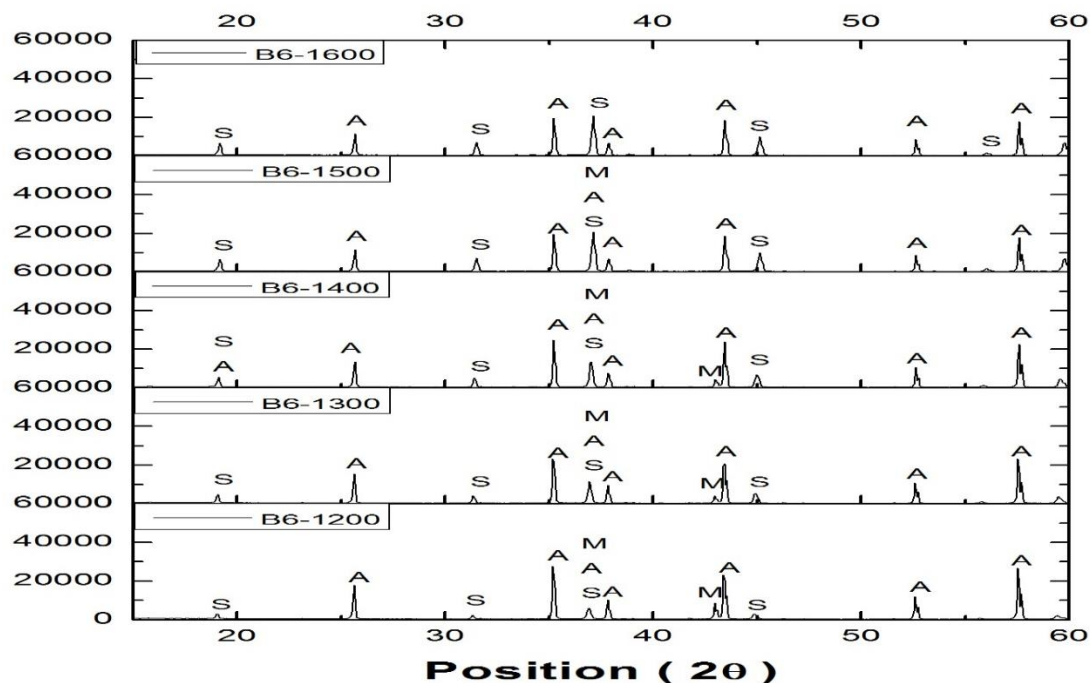


Figure 34 Comparison of XRD analysis plots of all B6 batch

The Fig. 23– Fig. 28 are showing the XRD analysis pattern of all the 80:20 batches and Fig. 29– Fig. 34 are showing the XRD analysis pattern of all the 90:10 batches where the denotations are as follows.

M - Periclase phase

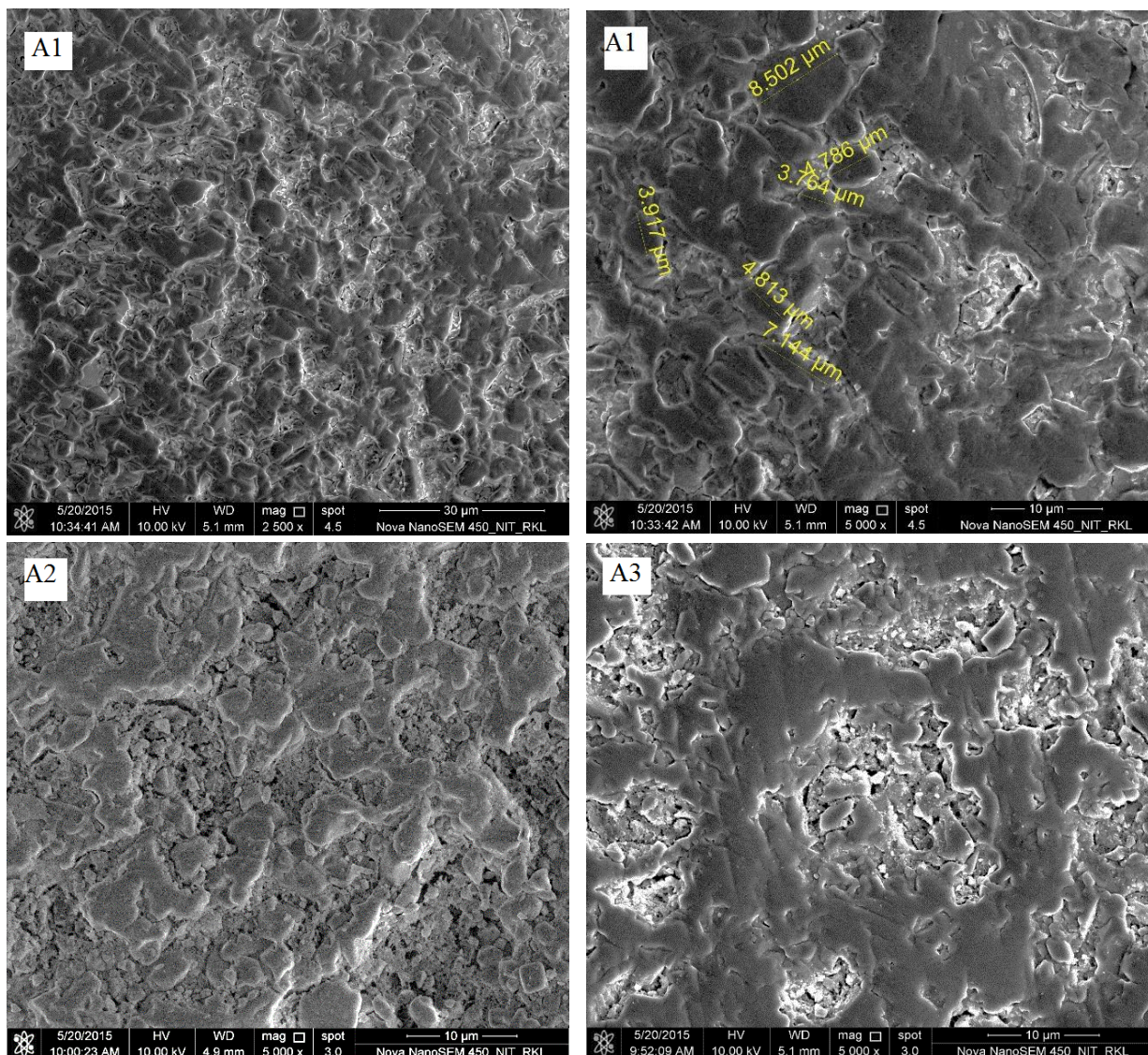
A - Corundum phase

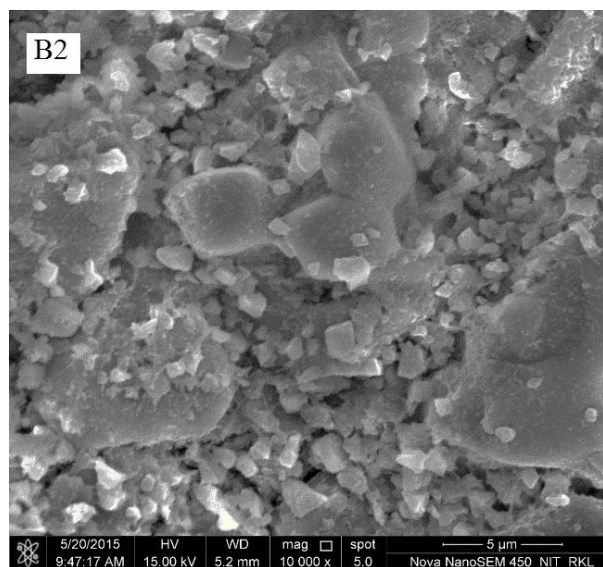
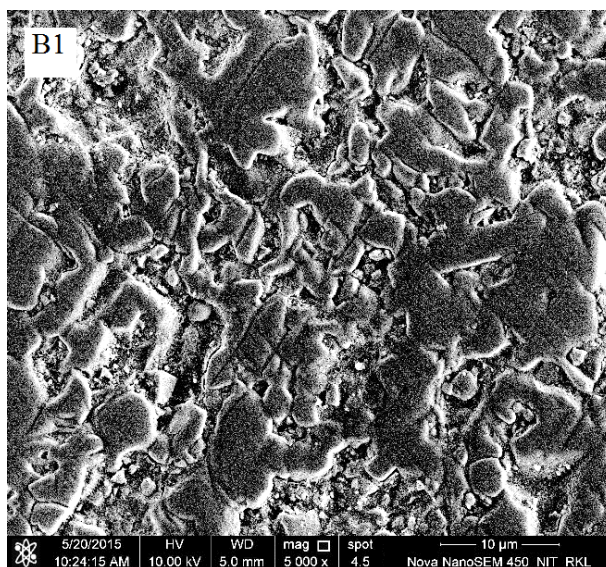
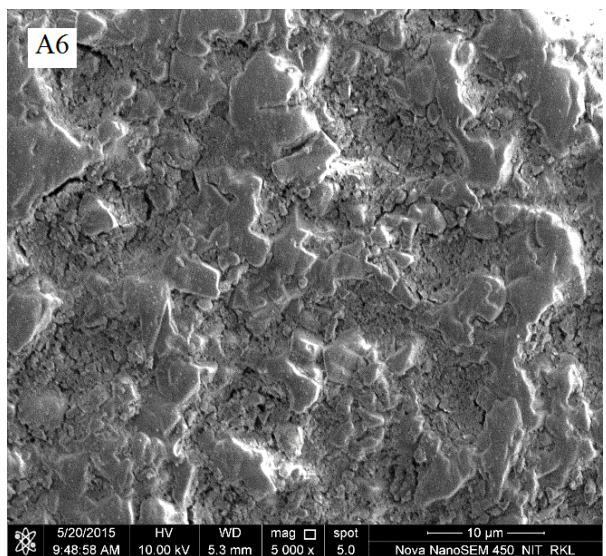
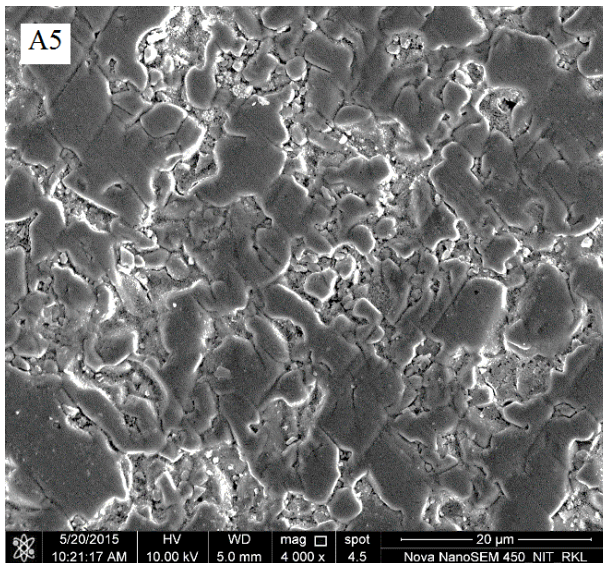
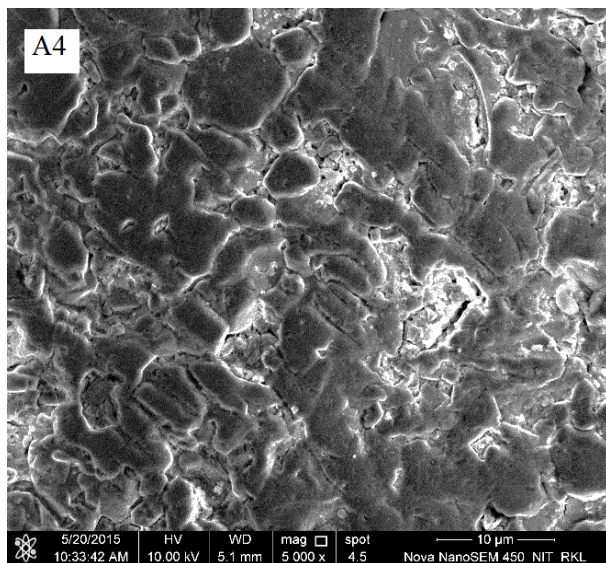
S – Spinel phase

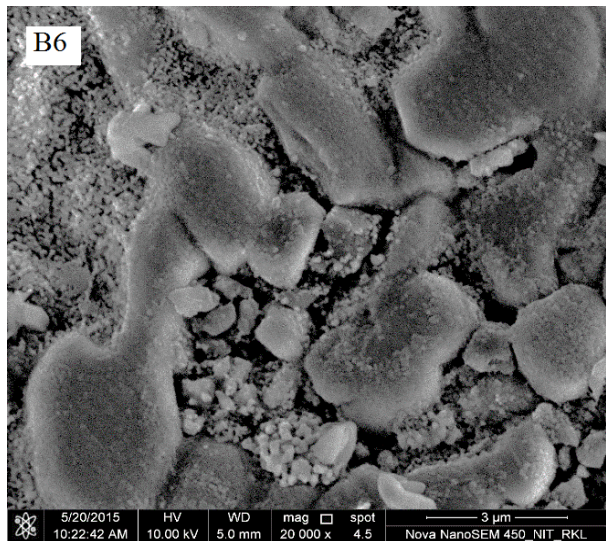
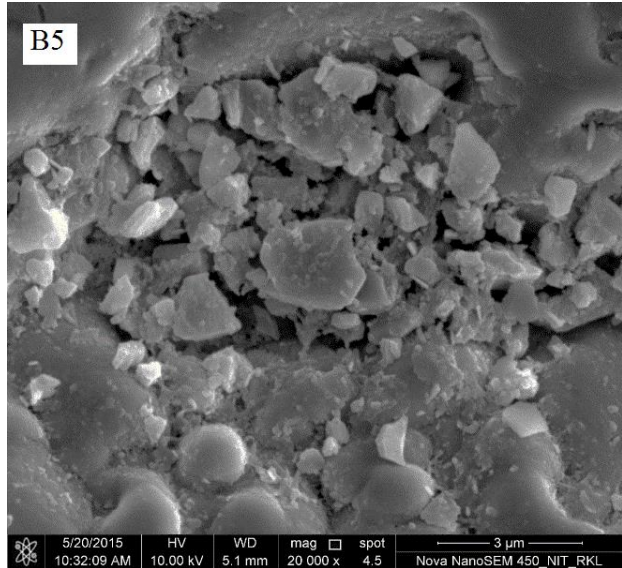
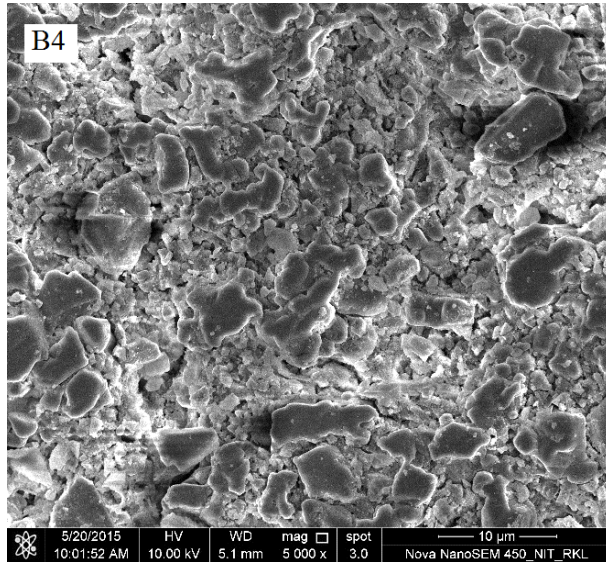
Spinel peaks could be observed in all of the batches sintered at 1200°C which means spinalization starts below this temperature. The intensity of the spinel peaks increased and that of magnesia and alumina decreased with increasing temperature which indicates that the spinel formation increases with increasing temperature by the reaction between magnesia and alumina.

The individual component (magnesia and alumina) peaks almost vanished for the 80:20 batch samples whereas they were present in case of the 90:10 batch, though in a minimal amount, even at 1600°C. Spinel peaks were not as significant in case of the B batches as in case of the A batches. This may be due to the lesser magnesia availability in B batch, for spinel formation and an excess of alumina, which has resulted for both the above phenomena.

FESEM Analysis:







The FESEM microstructures of all the batches sintered at 1600°C are shown in the above given figures. Microstructural study showed a well compacted microstructure of all the compositions of the A16SG containing compositions. All the A1, A4, B1 and B4 compositions showed (marked A1, A4, B1, B4) non-uniform distribution of different sized grains but the grains are very compact and showed very minimum porosity. This indicates the attainment of high sintered density values for the compositions.

Compositions containing CL 370 showed less compact microstructure with some amount of porosity in between the grains. The grains are also non uniform in size and there are regions of well compact areas and some areas with small grain with higher porosity. The figures marked as A2, A5, B2 and B5 are showing their corresponding photomicrographs.

Less or minimum compacted porous microstructure was observed for the compositions containing CT9FG alumina. The grains are non-uniform in size and are in less compact condition. Porosity among the grains are observed indicating poor sintering and densification of the compositions on sintering. Photomicrographs of A3, A6 and B6 are shown in figures marked as A3, A6 and B6.

One interesting phenomena was observed in the microstructure of the B compositions. Exsolution of alumina was observed in these compositions as small whitish particles, distributed in the microstructure. Alumina at higher temperature got dissolved in spinel structure due to higher solid solubility of alumina in spinel, but during cooling, the solid solubility got decreased and alumina comes out from the spinel grains as small exsolved phases. This phenomena is strong for the B compositions due to the higher content of alumina in the compositions.

Chapter 6

Conclusion

CONCLUSION:

- From the plots of linear dimensional change after firing, bulk density and apparent porosity, it can be concluded that, the batches with the finest alumina batch i.e. A16SG, have undergone maximum densification. This presents a very clear picture of a direct proportionality of fineness with densification.
- The presence of spinel phase peaks at 1200°C signified the beginning of the spinalization process below this temperature.
- Corundum phases almost disappeared in samples of 80:20 batches fired at 1600°C. However the corresponding batches of 90:10 composition were found to be associated with residual alumina peaks even at the highest firing temperature due to its excess amount content.
- The microstructures presented a somewhat clear idea about the compaction pattern of the samples which were again supported by their obtained BD values. Batches with A16SG as its component offered a denser picture than the other batches. Excess alumina appeared as small whitish particles in the 90:10 batch as an exsolved phase.

Chapter 7

References

REFERENCES:

- [1] Karisheff, A.De., “Refractory products and method of fabrication”. France Patent No. 350016 (1905) (refac-2010)
- [2] Bosh, P. and Giry, J. P., “Preparation of zirconia - mullite ceramics by reaction sintering. Science of Sintering”, 1988, 20, 141 - 148.
- [3] Ryshkewitch, E., Oxide Ceramics. Academic Press, New York (1960), 257–274 (refac-2010)
- [4] S. T. Murphy; C. A. Gilbert; R. Smith; T. E. Mitchell; R. W. Grimes, “Non-stoichiometry in MgAl_2O_4 spinel”, Philosophical Magazine, 90 [10] 1297-1305 (2010)
- [5] <http://www.slideshare.net/shivadheeraj/x-ray-diffraction>
- [6] <http://photometrics.net/analytical-techniques/field-emission-scanning-electron-microscopy-fesem>
- [7] Maschio, R. D., Fabbri, B. and Fiori, C., “Industrial applications of refractories containing magnesium aluminate spinel”. Industrial Ceramics, 1988, 8, 121 - 126.
- [8] Ritwik Sarkar and Goutam Banerjee, “Effect of Compositional Variation and Fineness on the Densification of $\text{MgO} \pm \text{Al}_2\text{O}_3$ Compacts”. Journal of the European Ceramic Society 19 (1999) 2893 - 2899.
- [9] Carter RE., “Mechanism of solid state reaction between $\text{MgO}-\text{Al}_2\text{O}_3$ and $\text{MgO}-\text{Fe}_2\text{O}_3$ ”. J Am Ceram Soc 1965; 44 (3) 116– 120
- [10] Ritwik Sarkar, Sachin Sahoo, “Effect of raw materials on formation and densification of magnesium aluminate spinel”, Ceramic International, 40[10] 16719 – 16725 (2014).
- [11] Bailey, J. T. and Russel, R., “Sintered spinel ceramics”. American Ceramic Society Bulletin, 1968, 47, 1025 - 1029.

- [12] Teoreanu, I. and Ciocea, N., “Magnesia-alumina spinel refractories”. Interceram., 1987, 4, 19 - 21.
- [13] Sarkar, R., Das, K., Das, S. K. and Banerjee, G., “Development of magnesium aluminate spinel by solid oxide reaction”. UNITECR-1997, Vol. II, pp. 1053 - 1058.
- [14] Bailey, J. T. and Russel, R., “Preparation and properties of dense spinel ceramics in the $\text{MgAl}_2\text{O}_4\pm\text{Al}_2\text{O}_3$ system Transaction & Journal of the British Ceramic Society, 1969, 68, 159 - 164.
- [15] Bailey, J. T. and Russel, R., “Magnesia rich MgAl_2O_4 spinel ceramics”, American Ceramic Society Bulletin, 1971, 50, 493 - 496.
- [16] Hing, P., “Fabrication of translucent magnesium aluminate spinel and its compatibility in sodium vapours”, Journal of Material Science, 1976, 11, 1919 - 1926.
- [17] Kenya, H., Tadashi, O. and Zenbee, N., Effect of starting materials and calcining temperature on the sintering of spinel ceramics. Rep. Res. Lab. Eng. Mater., Tokyo Ins. Tech., 1977, 2, 85±94.
- [18] C.-J. Ting and H.-Y. Lu, “Defect Reactions and the Controlling Mechanism in the Sintering of Magnesium Aluminate Spinel,” J. Am. Ceram. Soc., 82 [4] 841–8 (1999).
- [19] I. Ganesh, S.M. Olhero, A.H. Rebelo, J.M.F. Ferreira, “Formation and Densification Behavior of MgAl_2O_4 Spinel: The Influence of Processing Parameters”, J. Am. Ceram. Soc., 91 (2008), p. 1905.
- [20] S. Yangyuan, R.J. Brook, “Preparation and Structure of Forsterite-Zirconia Ceramic Composites”, Cer. Int., 9(2), (1983), 39-45.
- [21] M.A.L. Braulio a, M. Rigaud b, A. Buhr c, C. Parr d, V.C. Pandolfelli, “Spinel-containing alumina-based refractory castables”, Ceram. Int., 37 (2011), pp. 1705–1724.

- [22] N.A.L. Mansour, “Effect of Magnesia and Alumina Characteristics on the Formation of Spinel,” *Interceram*, **27** [1] 49–51 (1978).
- [23] E. Kostic, S. Boskovic and S. Kis, “Influence of Addition of Mechanical Energy on High-Temperature Processes in Solids”; pp. 319–26 in *Proceedings of the 4th European Ceramic Society Conference*, Vol. 2. 1995.
- [24] L.B. Kong, J. Ma and H. Huang, *MgAl₂O₄ Spinel Phase Derived from Oxide Mixtures Activated by a High-Energy Ball-Milling Process*,” *Mater. Lett.*, 56 [3] 238–243 (2002)
- [25] R. Sarkar, A. Ghosh and S.K. Das, “Reaction-Sintered Magnesia-Rich Magnesium Aluminate Spinel: Effect of Alumina Reactivity,” *Ceram. Int.*, **29** [4] 407–11 (2003).
- [26] J. Li, T. Ikegami, J. Lee, T. Mori and Y. Yajima, “A Wet Chemical Process Yielding Reactive Magnesium Aluminate Spinel (MgAl₂O₄) Powder,” *Ceram. Int.*, **27**, 481–89 (2001).